Hydrothermal processes

Christopher R German[a], Susan Q Lang[a], and Jessica N Fitzsimmons[b], [a]Woods Hole Oceanographic Institution, Woods Hole, MA, United States; [b]Texas A&M University, College Station, TX, United States

Abstract

Submarine hydrothermal activity was detected only toward the latter part of the 20th Century as a direct – but largely unanticipated – consequence of the Plate Tectonics Revolution. It has now been shown to occur in every ocean basin of our planet and to have profound impacts on ocean biogeochemical cycles. In the past decade, one particularly important advance has been the realization that we have not yet identified the full spectrum of geologic settings in which submarine venting can occur; hence, we have not yet characterized the full range of geochemical fluxes that can arise from hydrothermal circulation in the sub-seafloor. A further important discovery is that the release of trace elements and isotopes may be intimately associated with the global carbon cycle, not just at the deep seafloor but up to and including sequestration of significant amounts of carbon at the air-sea interface: in High Nutrient Low Chlorophyll (HNLC) regions at high latitudes, hydrothermally-sourced Fe may provide a previously unrecognized source of essential micronutrients to sustain primary productivity. Finally, the last decade has revealed the presence of multiple additional ocean worlds within our solar system, at least some of which have the capacity to host – and even have already revealed evidence for – styles of submarine venting that could support abiotic organic synthesis and, potentially, be inhabited.

Keywords

Astrobiology; Diffuse flow; Hydrothermal plumes; Hydrothermal vents; Ocean worlds; Water rock interactions

Key points

- Hydrothermal circulation is ubiquitous throughout Earth's oceans. It plays a major role in transporting heat away from the Earth's interior as part of the on-going plate tectonic cycle. While it has long been evident that such processes must have a consequential impact on ocean biogeochemistry, the full extent of that impact continues to be revealed.
- Of particular note has been the recent recognition that water-rock interactions do not just result in the supply of dissolved gases and ionic/inorganic species (e.g. dissolved metals and mineral precipitates) to the oceans but can also lead to the spontaneous generation of key organic compounds including those considered to be the putative "building blocks for life."
- Recent work using novel survey approaches has revealed an ever-expanding diversity of geologic settings that can host submarine venting, each with novel geochemical characteristics. They are found not just along mid-ocean ridges, but also at isolated seamounts, at arcs, back-arcs and even trenches associated with subduction zones. They could provisionally occur within transform faults as well.
- We now recognize that the impact of submarine hydrothermal circulation on ocean biogeochemistry may be more profound than previously recognized – even a decade ago. Two key findings contribute to this assertion: (i) sites of low-temperature flow, out of chemical (redox) equilibrium with the overlying water column, are far more numerous than the "black smoker" fields prospected for and identified in preceding decades; (ii) the geochemical influence of hydrothermal plumes extends much farther than previously anticipated, spanning entire ocean basins and, prospectively, even serving to fertilize primary productivity in HNLC regions of the surface ocean.
- Planetary environments with water-rock interactions and hydrothermal systems akin to those in Earth's oceans are now inferred or anticipated on multiple planetary bodies in our outer solar system. This offers the exciting prospect of habitability, in the form of chemosynthesis (as found at submarine vents) even in settings too distant from the Sun to offer much potential for photosynthesis (the process that fuels the majority of life on Earth). In the coming decade, NASA (together with other space agencies) is preparing to develop new missions to build on this hypothesis and explore for evidence for life beyond Earth, fueled by hydrothermal systems on ocean worlds in the outer solar system.

Introduction

What is hydrothermal circulation?

Submarine hydrothermal circulation occurs when a subsurface heat source (magma or hot, solid rock) drives seawater convection through the permeable oceanic basement. The seawater interacts with the fractured ocean lithosphere resulting in rock alteration and modified fluid compositions. Hydrothermal systems can arise in a diverse array of volcanic/tectonic regimes - wherever pathways exist for the intersection of subseafloor fluid flow with Earth's geothermal gradient. The phenomenon has received most attention to-date along the global mid-ocean ridge system where exciting new discoveries continue to be made. But submarine hydrothermal circulation can also occur in other geologic settings: in association with intra-plate volcanic hot-spots, at convergent margins (arcs, back-arcs, subduction zones) and, potentially, along transform faults and oceanic fracture zones.

In general, all hydrothermal circulation follows a common path in which cold and dense, downward-percolating seawater is first heated and then undergoes chemical modifications through a progressive series of reactions with host rocks, reaching maximum temperatures that can exceed 400 °C. The heated circulating fluids then become buoyant and rise rapidly back to the seafloor where, at their most spectacular, they are expelled undiluted into the overlying water column. A diversity of cooler hydrothermal fluids can also be found exiting the seafloor, however, with a variety of sources. They can result from mixing, just beneath the seafloor, between hot ascending fluids and cold seawater, or they can form as unmixed but more moderately heated fluids following different sub-seafloor trajectories. It has long been established that seafloor hydrothermal circulation plays a significant role in the cycling of energy and mass between the solid earth and the oceans (see, e.g., Schultz and Elderfield, 1997), but the focus of this chapter is upon the impact that such circulation can have on local-, basin- and global-scale ocean (bio)geochemistry.

The first identification of submarine hydrothermal venting and accompanying chemosynthesis-based communities in the late 1970s remains one of the most exciting discoveries in modern science. Continuing exploration has revealed surprising new discoveries in the decade since the last edition of the Treatise of Geochemistry, including: (a) demonstration that seafloor hydrothermal circulation can give rise to abiotic synthesis of key organic molecules critical to the origin of life; (b) revelation that hydrothermal plume discharge can fertilize primary productivity at high latitudes in Earth's sunlit upper oceans, impacting the draw down of atmospheric CO_2; and (c) discovery that submarine venting may be present on other ocean worlds in the outer solar system, potentially rendering them habitable and, thus, providing compelling new targets in the search for life beyond Earth.

The existence of some form of seafloor hydrothermal circulation was predicted almost as soon as plate tectonics theory emerged (Lister, 1972). When compared to predicted *conductive* heat-fluxes across mid-ocean ridges, it soon became apparent that significant heat must, instead, be extracted from young ocean crust through *convection*, with the "missing" heat being transported by some form of submarine hydrothermal circulation (Fig. 1). Preliminary evidence that such processes might have a geochemical as well as a geophysical signature came with the discovery of warm (40–60 °C) salty water in the deep rift basins of the Red Sea, underlain by thick layers of metal-rich sediment (Bischoff, 1969). Similar metalliferous core-top sediments were then found to be concentrated all along the newly-recognized global mid-ocean ridge system (Boström et al., 1969) (Fig. 2). Another early indication of hydrothermal activity came from the detection of plumes of excess ^{3}He in the Pacific Ocean (Clarke et al., 1969; Lupton and Craig, 1981) which could be sourced only through active degassing at the seafloor, from Earth's interior.

In 1977, scientists diving at the Galapagos Spreading Center reported the first direct evidence of hydrothermal fluids discharging chemically-altered seawater from young volcanic seafloor, at temperatures up to 17 °C (Edmond et al., 1979). Two years later, the

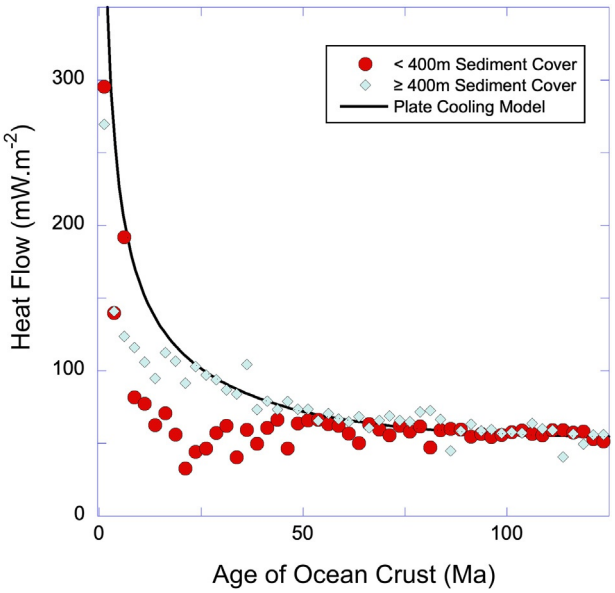

Fig. 1 Oceanic heat flow vs age of ocean crust (after Stein and Stein, 2015). Data from the Pacific, Atlantic, and Indian Oceans depart from the theoretical curve for cooling by conduction only (solid line: Hasterok, 2013a). Note that the evidence for additional convective cooling (conductive heat flow deficit from the plate cooling model) for young ocean crust is both more pronounced for lightly sedimented ridge-flanks (red circles) than for those with thick sediment cover (blue diamonds) and persists for greater distances (ages) off-axis (Hasterok, 2013b).

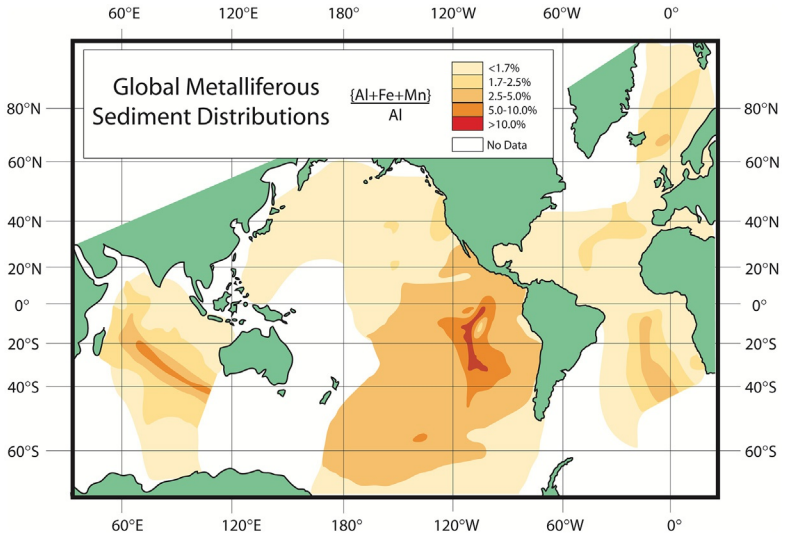

Fig. 2 Global map of the (Fe + Mn + Al):Al ratio, a tracer of metalliferous sediments, within surficial marine sediments. Highest ratios mimic the trend of the global mid-ocean ridge axis. After Boström et al. (1969).

first high-temperature (380 ± 30 °C) "black smoker" vent fluids were found at 21°N on the East Pacific Rise (Spiess et al., 1980) – with fluid compositions remarkably close to those predicted from the Galapagos findings (Edmond et al., 1982). Since that time, sites of seafloor venting have been identified along the global mid-ocean ridge system in every ocean basin – throughout the Pacific, Atlantic, and Indian Oceans (Beaulieu et al., 2013, 2015) and, in the past decade, even into the remote Southern Ocean (Rogers et al., 2012) and the ice-covered Arctic (German et al., 2022a).

It is now estimated that up to ~10 TW of cooling (~25% of Earth's global heat flow) occurs through submarine hydrothermal circulation, predominantly at mid-ocean ridges, where heat-flow data from throughout the world's ocean basins (Fig. 1) indicate that convective cooling plays an important role for ocean crust up to 75 Ma in age (Stein and Stein, 1994). The on-axis (0–1 Ma crust) component of this heat flux is relatively small (~2 TW) whereas the vast majority (~8 TW) occurs in the form of ridge-flank circulation through ocean crust 1–75 Ma in age (Mottl, 2003). Hasterok (2013a,b) has estimated that of the ~8 TW of heat flux associated with ridge-flank circulation (1–75 Ma) only ~0.2 TW may be associated with thick sediment cover (≥400 m) while the vast majority arises from circulation through young ridge-flanks with thin sediment cover (<400 m). This is important because it is only at ridge flanks covered by thick sediment that warm crustal reaction temperatures and anoxic basement fluids have been observed, but such thickly sedimented systems are considered too rare to be considered representative of global-scale ridge-flank hydrothermal geochemical fluxes (Mottl, 2003).

In stark contrast to ridge-flank systems, the most spectacular manifestations of seafloor hydrothermal circulation yet observed are the high-temperature (≥350 °C) vents that expel fluids from the seafloor, all along the global mid-ocean ridge axis. In addition to being visually compelling, high temperature vent fluids also exhibit important enrichments and depletions when compared to ambient seawater. Many of the dissolved chemicals released during subseafloor water-rock reactions precipitate upon mixing with the cold, overlying ocean, generating thick columns of black metal-sulfide and -oxyhydroxide mineral-rich fluids that visually resemble smoke – hence the colloquial name for these vents: "Black Smokers" (Fig. 3). Despite their common appearance, high-temperature hydrothermal vent fluids exhibit a wide range of temperatures and chemical compositions, which are determined by subsurface reaction conditions. While spectacular, high-temperature vents may represent only a small fraction of the total hydrothermal heat-flux from young (0–1 Ma) ocean crust along mid-ocean ridge axes. Instead, on-axis hydrothermal fluxes may be dominated by much lower-temperature fluids exiting the seafloor at temperatures comparable to those first observed at the Galapagos vent-sites in 1977 (Elderfield and Schultz, 1996; Mottl, 2003). Using conservative tracers, it has been estimated that, globally, some 20% of the heat available at mid-ocean ridges (0–1 Ma) is released, *on average*, via high-temperature black-smoker venting (Nielsen et al., 2006). How that flow is partitioned along slower versus faster spreading ridges, however, and what implications that might have for biogeochemical fluxes to the oceans are topics of on-going research; this is the major focus of the Section "The geo-diversity of submarine hydrothermal circulation" in this review.

While high-temperature vents represent only a small fraction of the total hydrothermal heat flux from young oceanic crust, they transport many inorganic and organic species into the water column. The buoyancy of the high-temperature vent-fluids causes them to rise from the seafloor entraining and mixing with ambient seawater until they eventually reach a level of neutral buoyancy, typically 100 m or more above the seafloor. As these plumes disperse, the processes active within them play an important role in determining the *net* impact of hydrothermal circulation upon the oceans and marine (bio)geochemistry; that is the subject of the Section "Hydrothermal interactions with the oceanic water column. In addition, it has been demonstrated that warm fluids, out of

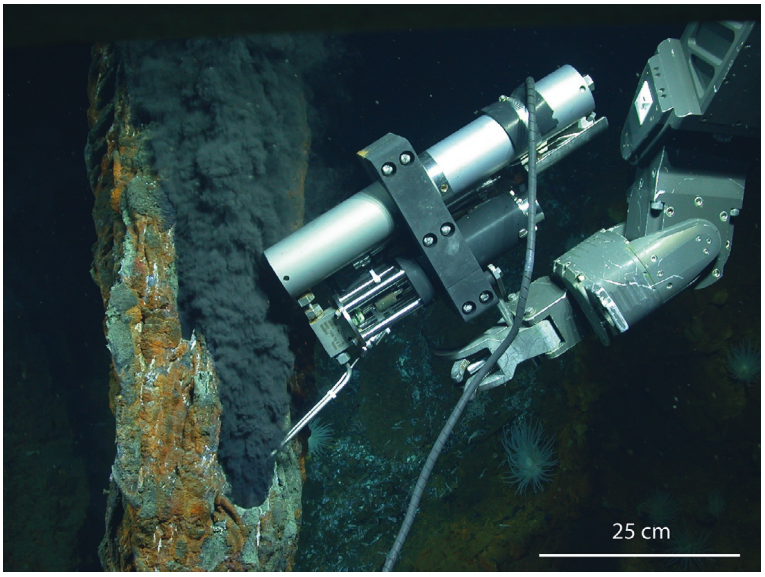

Fig. 3 Photograph of a "black smoker" hydrothermal vent emitting hot (395–400 °C) fluid at a depth of ~5000 m and being sampled using an Isobaric Gas-Tight Sampler using the ROV *Jason* at the Piccard hydrothermal field, Mid Cayman Rise. Photo Credit: C. German & ROV Jason; © WHOI.

geochemical equilibrium with the overlying ocean, may also be escaping from the seafloor at many more locations than just "Black Smokers" (Baker et al., 2016; Chen et al., 2020). Whether they are entrained into the upflow of hydrothermal plumes or not, those systems may also be playing an important role in regulating ocean biogeochemistry.

Where does hydrothermal circulation occur?

Hydrothermal circulation occurs predominantly along the global mid-ocean ridge crest, a near-continuous volcanic chain that extends over ~60,000 km (Fig. 4). Submarine hydrothermal activity is also now known to be associated with back-arc spreading centers formed behind ocean-ocean subduction zones and at intra-plate "hot-spot" volcanoes such as Hawai'i. As exploration continues, InterRidge sustains an updated list of known submarine vent-sites at https://vents-data.interridge.org. As an illustration of the rate at which vents continue to be discovered, Fig. 4 contains 135 new sites that were discovered in just the past decade (Beaulieu et al., 2013; Beaulieu and Szafranski, 2020).

In the first two decades following discovery of venting, a pattern emerged in which the frequency with which hydrothermal plume anomalies were detected along mid-ocean ridges in the eastern Pacific were found to scale with spreading rate – a convenient proxy for time-integrated magmatic heat budgets in young (0–1 Ma) ocean crust (Baker et al., 1996). With continuing exploration of slower spreading ridges in the Atlantic, Indian, and Arctic Oceans, however, this linear relationship was found to break down (Baker and German, 2004; Baker et al., 2004) with the "excess" venting at slow spreading ridges attributed to tectonically-controlled, rather than neovolcanically-controlled, high-temperature venting (German et al., 2016a). Along medium- and fast-spreading ridges the abundances of lower temperature venting identified in the most recent decade have brought into question whether our plume-prospecting techniques are adequate to reveal all the biogeochemically active sources of hydrothermal flow (see Section titled "The biogeochemical significance of low-temperature axial venting"). Continuing investigations will be required to evaluate this hypothesis and to reveal whether similar partitioning between high- and low- temperature venting occurs along slow and ultra-slow spreading ridges. It is certainly the case that at least one entirely different class of lower temperature submarine venting occurs along slow and ultra-slow spreading ridges (see Section "Ultramafic influenced venting").

Why should hydrothermal fluxes be considered important?

The impact of submarine venting on ocean chemistry has been evaluated many times since venting was first discovered (e.g., Edmond et al., 1979, 1982; Staudigel and Hart, 1983; Von Damm et al., 1985a; Elderfield and Schultz, 1996; Davis et al., 2003; Mottl, 2003; Nielsen et al., 2006; Vance et al., 2009; German et al., 2015, 2016b; Humphris and Klein, 2018). If all the heat released from the crystallization and cooling of basaltic magma at young (0–1 Ma) mid-ocean ridges were transported as high-temperature hydrothermal fluids (350 °C and 350 bar), the corresponding black smoker volume flux has been estimated at $5–7 \times 10^{16}$ g yr^{-1} (Elderfield and Schultz, 1996). The same study, however, also recognized that high-temperature hydrothermal fluids are unlikely to be entirely responsible for the transport of all axial hydrothermal heat flux. Based on a mass balance for Tl, for

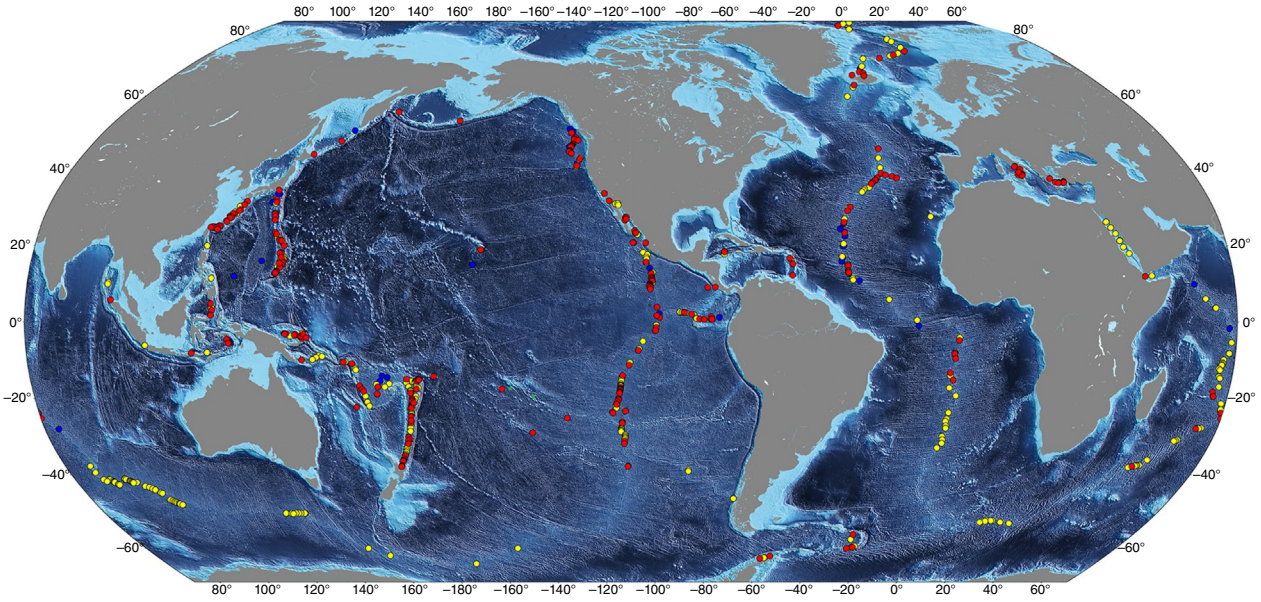

Fig. 4 Shaded relief of the ocean floor overlain by locations at which hydrothermal vents have already been located (red symbols) or inferred from the detection of diagnostic plume signals (yellow symbols). Updated from Beaulieu and Szafranski, 2020. A continuously updated listing of known hydrothermal vent sites and detected plume sources is maintained by the InterRidge program at: https://vents-data.interridge.org.

example, it has been estimated that the high-temperature fluid flux to the oceans may be significantly lower (0.17 to 2.93×10^{16} g yr^{-1}), with as little as 20% (range: 5–80%) of axial heat flux being transported in high-temperature fluids (Nielsen et al., 2006). Note, however, that such "global ocean" budgets, when based on single tracers, have the potential to yield large error bars.

To put hydrothermal volume fluxes in context, while the maximum flux of cool hydrothermal fluids on unsedimented ridge flanks may be comparable to global riverine water fluxes ($3.7–4.2 \times 10^{19}$ g yr^{-1}; Palmer and Edmond, 1989), high-temperature fluid fluxes at mid-ocean ridge axes may be ~1000-fold lower. Nevertheless, for an ocean volume of ca. 1.4×10^{24} g, this still yields a (geologically-short) oceanic residence time, with respect to high-temperature circulation, of ca. 20–30 Ma. This means that high-temperature fluid fluxes should be important for all elements that exhibit concentration changes more than 1000-fold greater than river waters. Further, high-temperature fluids entrain large volumes of ambient seawater into their buoyant and neutrally buoyant plumes (see Section "Hydrothermal interactions with the oceanic water column") with typical dilution ratios of ca. 10^4:1 (Lupton, 1995). Thus, if 20% of the fluids circulating at high temperature through young ocean crust were emitted at high temperature (1.2×10^{16} g yr^{-1}), the total water flux cycled through their overlying hydrothermal plumes should be of the order of 1×10^{20} g yr^{-1}. Not only does this flux exceed the global freshwater riverine flux, but the associated residence time of the global ocean, with respect to cycling through hydrothermal plume entrainment, would be $\leq$10 kyr and, hence, comparable to the timescale for the thermohaline circulation (Broecker and Peng, 1982). From that perspective, we can anticipate that hydrothermal circulation should play an important role in the marine biogeochemical cycle of any tracer that exhibits an oceanic residence time of >1–10 kyr.

Controls on the geochemistry of submarine vent fluids

The chemistry of submarine vent fluids is controlled by complex combinations of water-rock reactions, phase separation, biological activity, and mantle degassing (reviewed in Von Damm, 1995). Given the heterogeneity of fluid pathways through the subseafloor, perhaps it is not surprising that almost no two vent fluids have identical chemical compositions. Even the geochemistry of a fluid from a single location can change over time due to magmatic and tectonic events. Despite this complexity, some of the major reactions that control fluid chemistry are ubiquitous. Further, the unique fingerprint of a vent fluid can be used to infer the subseafloor conditions that it underwent during its journey.

Early insights into the controls on vent fluid chemistry came from laboratory experiments that allowed fluid geochemistry predictions to be made prior to the discovery of hydrothermal vents. Rock types comprising the oceanic lithosphere, such as basalt and peridotite, were reacted with seawater at elevated temperatures and pressures (Bischoff and Dickson, 1975; Hajash, 1975; Bischoff and Seyfried, 1978; Seyfried and Dibble, 1980), and showed that SO_4 and Ca are rapidly removed from fluids due to anhydrite precipitation (Fig. 5). Concentrations of Mg drop to near-zero due to rock alteration reactions, with an accompanying

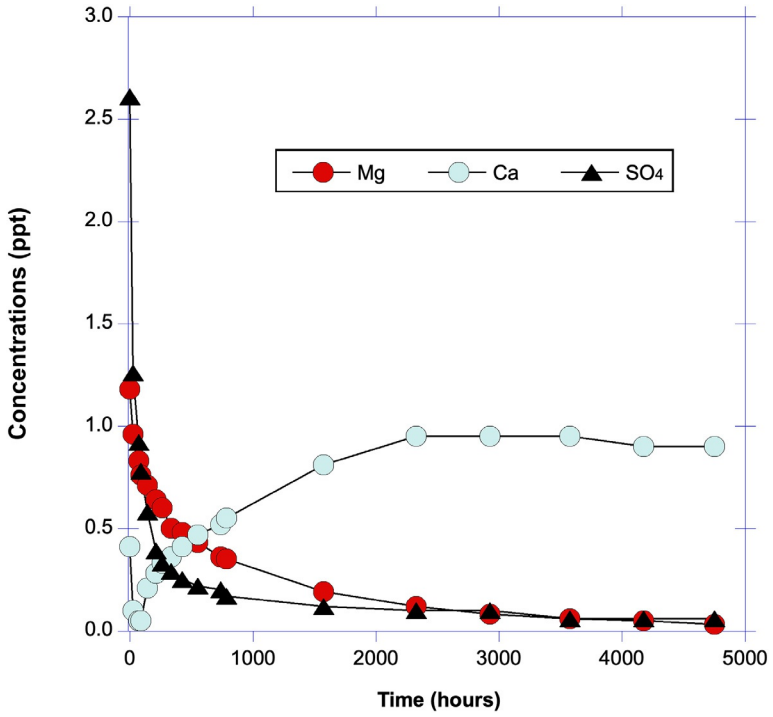

Fig. 5 Results from early laboratory experiments in which seawater was reacted with basalt powder at 200 °C, 500 bar (data from Bischoff and Dickson, 1975).

increase of Ca that ultimately raises its concentrations to higher than starting seawater (Bischoff and Dickson, 1975; Hajash, 1975; Bischoff and Seyfried, 1978). In basaltic systems, the H^+ ions liberated during these and other reactions cause fluids to be acidic at room temperatures. Altered fluids contain elevated concentrations of Si and trace metals such as Fe, Mn, and Cu that are leached from the basalt.

$$Ca^{2+} + SO_4{}^{2-} = \text{anhydrite } (CaSO_{4(s)}) \quad (1)$$

$$\text{Plagioclase} + Mg^{2+} + H_2O = \text{clays} + Ca^{2+} + K^+ + H_4SiO_4 + H^+ + Fe^{2+} + Mn^{2+} \quad (2)$$

The discovery of hydrothermal activity on the Galapagos Rift, hosted in basalts, provided the ultimate proof of these reactions occurring at spreading centers (Corliss et al., 1979; Edmond et al., 1979). Geophysical modeling of basement temperatures provided estimates of how much heat must be lost from the crust due to circulating fluids. Now that these fluids could be sampled directly, the ratios of elemental concentrations to heat (derived from fluid temperature) could be extrapolated to total global geochemical fluxes (Corliss et al., 1979). From these calculations it was immediately clear that hydrothermal circulation is responsible for removing large quantities of Mg from the ocean.

The earliest recognized hydrothermal systems were hosted in young crust at spreading centers, leading some to believe further exploration was unnecessary as all systems would reflect the reaction between two relatively uniform materials: hot basaltic ocean crust and seawater. Over time, however, our access to the deep sea has expanded and the incredible diversity of rock types, temperatures, pressures, and residence times that fluids are exposed to during transit through the oceanic basement has become more apparent. Below, we briefly summarize some of the major processes that impact fluid geochemistry. In the following section we discuss the major known types of hydrothermal systems and their associated geochemistry.

In general, fluids percolate into the crust, react with the host rock at elevated temperatures, then rise buoyantly to exit at the seafloor. Close to the point where fluids exit the seafloor, local seawater often mixes in the near-subsurface to create lower temperature 'diffuse' vents (Fig. 6). While such conceptual diagrams may depict subseafloor hydrothermal systems in a 'flow-through' context, with a steady progression from deep recharge to upflow, it is likely that fluid flow through the subseafloor is more complex and heterogeneous, with packets of fluids trapped in pore spaces for variable amounts of time before mixing back into a main flow path. Thus, fluids that exit the seafloor reflect an integration of all the reactions that occur along that pathway.

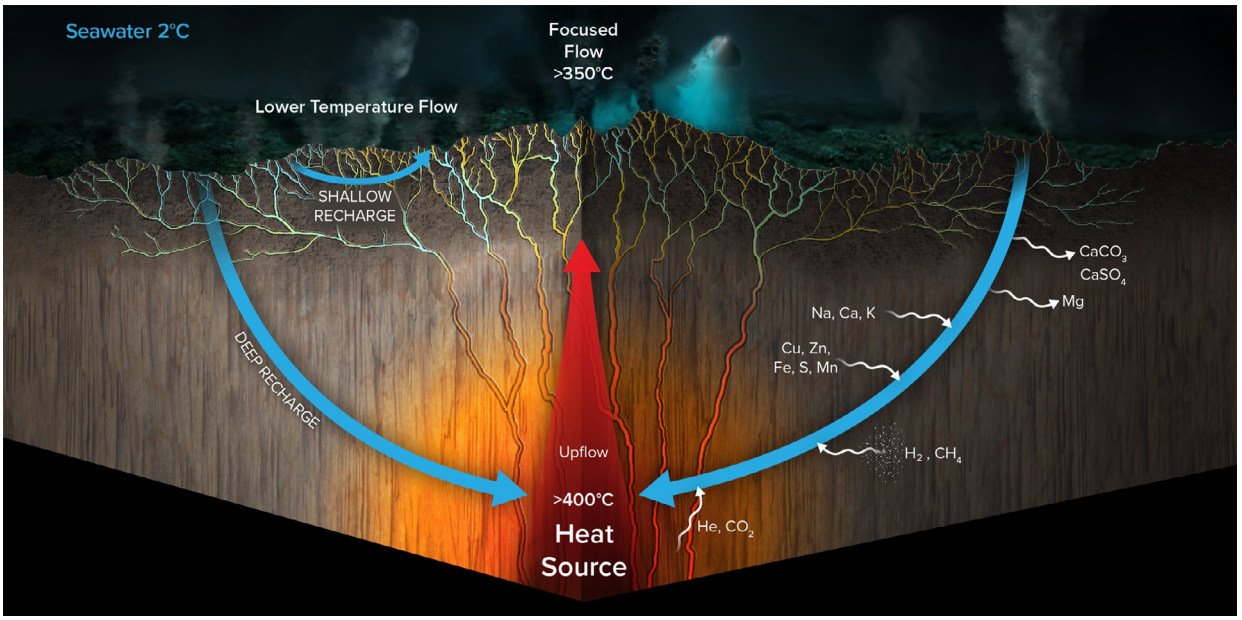

Fig. 6 Idealized cross section of a hydrothermal system. Seawater enters the basaltic crust through cracks and fissures in the seafloor and undergoes a series of water-rock interactions that cause large elemental changes, including the loss of Mg and the gain of trace metals. Magmatic degassing may contribute volatiles such as He and CO_2. If the fluid reacts with ultramafic (mantle) rocks, H_2 may be generated. Fluid inclusions and pore spaces within plutonic rocks contain a variable mix of CH_4, H_2, CO_2, and other volatiles that can be mobilized by circulating fluids. When heated to temperatures >300 °C, fluids undergo phase separation, creating both a volatile-rich and a brine-rich fluid. The hot fluids rise buoyantly and exit at the seafloor through focused, high temperature hydrothermal chimneys or via more widespread exit points after conductive cooling. Low temperature (diffuse flow) venting can arise either through near-subseafloor mixing between high temperature fluids and seawater, or from shallow recharge and low-temperature water rock reactions that never reach the hottest temperatures associated with black smoker venting.

Water-rock reactions

Inorganic geochemistry

The reactions that occur between rocks and seawater at elevated temperatures fundamentally set the geochemistry of hydrothermal vent fluids. Deep seawater is largely geochemically uniform, so much of the variation in fluid geochemistry is driven by host rock type and the temperature of the system. The oceanic lithosphere is composed of both mafic rocks, such as basalt and gabbro, and ultramafic rocks, such as peridotite. Fast and intermediate spreading centers with a robust supply of magma are dominated by mafic rocks. At slow and ultraslow spreading centers, ultramafic rocks from deeper in the lithosphere are exhumed and can be exposed along significant parts of the mid-ocean ridge. Fluids that percolate through sediments are further modified through reactions with terrigenous and/or photosynthetically derived materials.

Some reactions occur independent of host rock type. Anhydrite ($CaSO_4$) precipitation proceeds simply by heating seawater to temperatures >140 °C, and Mg is removed from solution in the form of Mg-hydroxy-silicates. Oxygen and other oxidants are rapidly removed due to microbial processing and/or redox reactions with minerals. As a result, fluids are highly reducing; sulfur is typically present as hydrogen sulfide (H_2S) or elemental sulfur (S^o), nitrogen as ammonia or ammonium.

In mafic systems, reacting fluids become acidic and rich in dissolved trace metals. Sodium is lost and calcium gained due to Na—Ca replacement reactions in plagioclase minerals (albitization). Potassium and other alkalis undergo similar reactions that generate acidity. Large quantities of iron, manganese, and silicon are leached out of rocks and into fluids. The bicarbonate that dominates seawater can be precipitated as calcium carbonate; the extent to which this reaction proceeds depends in part on the temperatures, pH, and alkalinity of the fluids (Alt et al., 2013; Coogan and Gillis, 2018). One of the few ions that is largely unreactive is chloride as it has almost no mineralogic sink. The concentration of Cl therefore provides an important tracer of other physical processes such as phase separation and hydration/dehydration reactions.

Ultramafic rocks contain substantial amounts of olivine and pyroxene that undergo a reaction called serpentinization when exposed to seawater (Früh-Green et al., 2004). The rock takes up water and releases OH^- and H_2, resulting in fluids that are more alkaline than mafic systems and rich in the dissolved gases H_2 and CH_4. Ultramafic systems with minimal magmatic input, such as Lost City, tend to have very low concentrations of trace metals such as iron and manganese and do not reach the high temperatures (>300 °C) of magmatic systems (Kelley et al., 2005). Many vent fields exist, however, such as the Rainbow hydrothermal field, that exhibit attributes of both ultramafic (e.g., high H_2) and mafic (e.g., high temperatures, high trace metals) influence (Charlou et al., 2010). Clearly, vent fluid geochemistry can occur in a continuum between idealized endmembers.

Abiotic synthesis and alteration of organic compounds

Hydrothermal fluid geochemistry has historically been focused on the large compositional changes to inorganic species and volatiles, but water-rock interactions also impact the organic geochemistry of fluids in unique ways (Lang et al., 2019). Deep seawater carries 34–48 μM of refractory dissolved organic carbon that is largely removed during circulation through high temperature and ridge flank hydrothermal systems (Lang et al., 2006; Lin et al., 2012; Shah Walter et al., 2018), constituting a significant global sink (Shah Walter et al., 2018). In lower temperature subseafloor systems, chemoautotrophic microbial communities synthesize new organic material that is exported to the deep sea (Lang et al., 2006; McCarthy et al., 2011). Hot fluids that interact with sediment cause the alteration and break down of biologically derived compounds, creating small soluble organics as well as larger, insoluble oil-like material that accumulates in the solid phase (Kawaka and Simoneit, 1987; Seewald et al., 1990; Lin et al., 2017). The organic compounds produced in hydrothermal systems can bind to the trace metals leached into the fluids, facilitating their solubility in the water column and their transport across ocean basins (Bennett et al., 2008; Sander and Koschinsky, 2011).

Perhaps the most exciting development over the past 15 years, however, is the recognition of wide-spread abiotic synthesis of organic molecules in hydrothermal settings. The H_2 produced by serpentinization and other types of fluid-rock interactions can react with inorganic carbon to form methane and short chain hydrocarbons by the general reaction (McCollom and Seewald, 2007):

$$CO_2 + H_2 \rightarrow CH_4 + C_2H_6 + C_3H_8 + C_nH_{n+2} \ldots . + H_2O \quad (3)$$

Abundant (milli-molar) concentrations of abiotic methane are a signature of ultramafic systems (Charlou et al., 2010; Proskurowski et al., 2008). The formation of CH_4 from CO_2 is kinetically inhibited at temperatures <300 °C (McCollom and Seewald, 2007; McCollom, 2016), which is hotter than several modern systems with elevated CH_4 concentrations (e.g., Lost City, Von Damm), suggesting that methane may not be synthesized on the timescales of active circulation. Instead, CH_4 may form during earlier, hotter stages of hydrothermal systems, trapped in fluid inclusions, and only later be released into circulating fluids (see Section "Magmatic degassing of volatiles", below).

The single carbon organic acid formate (HCOOH) rapidly equilibrates abiotically with CO_2 and H_2 and has also been identified in multiple ultramafic and subsurface systems at micro-molar to milli-molar concentrations (Lang et al., 2010; McDermott et al., 2015; Sherwood Lollar et al., 2021). Trace concentrations of methanethiol (CH_3SH) have also been reported from many types of hydrothermal fluids (Reeves et al., 2014), and the amino acid tryptophan and structurally similar organic molecules have more recently been identified in association with serpentine alteration phases recovered from ocean drilling (Ménez et al., 2018). The abundance and diversity of abiotic organic molecules in hydrothermal systems has raised the possibility that these environments could have provided the prebiotic soup necessary for the emergence of early life (Baross et al., 2019).

Phase separation

At high temperatures and pressures, hydrothermal fluids will undergo phase separation in the form of either separation into a low-salinity vapor phase and a brine phase or, if phase separation occurs above the critical point of seawater, a small amount of high salinity brine condenses from the fluid. In either case, two conjugate fluids result, and chemical species will preferentially separate into either the brine or the vapor phase depending on their affinity. Metals and non-volatile elements such as Cl will preferentially remain in the brine phase, with most cations maintaining their element-to-Cl ratios (Butterfield et al., 1994). Volatiles such as H_2, CH_4, H_2S, He, and CO_2 will partition into the less dense vapor phase. The temperature at which phase separation occurs depends on fluid salt content and pressure, so vents hosted at greater depths can be heated to more extreme temperatures before undergoing phase separation. The resulting impacts on vent-fluid composition can be significant, with Cl contents reported as much as 10 times lower than seawater (Von Damm et al., 1995). Essentially no fluids reported from any mafic hydrothermal systems have been found to exhibit chlorinities equal to local ambient seawater, indicating that phase separation is a ubiquitous process (Edmonds and Edmond, 1995). For a more extensive treatment of phase separation, the reader is directed to prior versions of this chapter (German and Von Damm, 2004; German and Seyfried, 2014).

Magmatic degassing of volatiles

Hydrothermal circulation is intimately associated with the magmatic processes that form new oceanic crust and is the primary mechanism that transfers heat and elements from the lithosphere to the overlying ocean. Seismic surveys have identified magmatic bodies underlying vent fields on fast and intermediate spreading centers (e.g., Singh et al., 1998; Robinson et al., 2020), some of which are periodically resupplied with fresh material (Wilcock et al., 2016). As magma ascends and cools, the decrease in pressure and temperature lowers the solubility of dissolved volatiles (H_2O, CO_2, ^3He), causing the formation of a gas phase that can be entrained into hydrothermal fluids (Fyfe et al., 1978). Mantle-derived ^3He is used as a local and ocean basin-wide tracer of hydrothermal plume processes (see later Section "Hydrothermal interactions with the oceanic water column"). The vast majority of high temperature hydrothermal fluids have CO_2 concentrations equal to or greater than deep seawater due to magmatic CO_2 inputs (McCollom, 2008). Natural abundance $^{14}C—CO_2$ has been used to track local processes such as magmatic events and the incorporation of mantle carbon into food webs (Proskurowski et al., 2004; Lang et al., 2018).

Not all magmatic gases are released immediately into hydrothermal systems. As melts cool and primary minerals undergo alteration, gases can also be trapped in the form of vesicles, stored over geologic time scales and, under favorable physicochemical conditions, the trapped CO_2 can subsequently be re-speciated into CH_4 and graphite (Kelley and Früh-Green, 2001). It has been proposed that the abundant CH_4 associated with ultramafic systems may also be due, at least in part, to the remobilization of CH_4 that re-speciated from magmatic CO_2 in fluid inclusions formed at high temperatures (Kelley and Früh-Green, 2001; McDermott et al., 2015; Klein et al., 2019).

Subseafloor residence times

The amount of time that fluids spend in the subseafloor, referred to as their subseafloor residence time, will also influence the extent to which slower water-rock reactions proceed. Fluids in high temperature hydrothermal systems percolate into the crust, are heated in the subseafloor, and buoyantly rise to return to the seafloor on time scales of <1 year (Kadko and Moore, 1988; Moore et al., 2021). This rapid rate of ascent is often used to infer pressure conditions at the base of hydrothermal circulation cells from Si concentrations in sampled fluids, assuming the latter reflect equilibration with quartz at high temperature (Foustoukos and Seyfried Jr., 2007). In ridge flank systems, water continues to circulate through older crust at lower temperatures. Fluid pathways are longer, and residence times can reach decades to thousands of years (Elderfield et al., 1999; Neira et al., 2016). As an example of how residence times impact fluid chemistry, chemical species such as magnesium are largely unreactive over short time periods at temperatures $<150\ ^\circ C$ (Seyfried and Bischoff, 1979). The fluids on the Juan de Fuca ridge flank are $<65\ ^\circ C$ but lack any dissolved Mg (Mottl et al., 1998); the long residence times allow alteration reactions to occur that are too slow to be observed on the timescale of laboratory experiments (Fisher and Wheat, 2010).

Temporal variability

Within single vents, the fluid composition can change significantly over relatively short timescales (minutes to years) due to geotectonic variations that can affect any of the variables listed above. This temporal variability has been studied very well at EPR 9°N (Von Damm, 2000; Escartin et al., 2007; Tolstoy et al., 1996) following magmatic events in 1991 and 2005–2006, as well as Main Endeavor Field on the Juan de Fuca Ridge in 1999 (Lilley and Von Damm, 2008; Lilley et al., 2003) and Kama'ehuakanaloa (Lo'ihi) in 1996 (Wheat et al., 2000). In contrast, other sites, especially those with little to no magmatic activity, exhibit remarkably constant vent fluid compositions; the best example of this is the TAG site on the slow-spreading Mid-Atlantic Ridge, which has exhibited stable vent fluid compositions for several decades (Gamo et al., 1996; Chiba et al., 2001).

Biological influence on fluid geochemistry

Microorganisms have been found to proliferate in subseafloor hydrothermal systems regardless of geologic setting. Although hydrothermal fluids are rich in trace metals and volatiles such as hydrogen and methane, they often lack other constituents

necessary for growth, such as nutrients. Zones where reduced hydrothermal fluids mix with oxidized seawater, therefore, represent ideal conditions for microbial metabolisms to exploit. In such mixing zones, strong redox gradients arise in which oxidized chemical species (e.g. O_2, CO_2, sulfate, nitrate) mix with reduced species (e.g. H_2, CH_4, H_2S). This causes thermodynamic disequilibria that can fuel microbial metabolisms such as sulfate reduction, methanogenesis, methanotrophy, and hydrogen oxidation (Amend et al., 2011; Dick et al., 2013; McCollom, 2000). The taxonomic and functional distribution of microorganisms is highly dependent on the host fluid chemistry, particularly pH, temperature, and the availability of reduced chemical species (Schrenk et al., 2010; Orcutt et al., 2011). Mixing zones can occur in the rocky subseafloor or in hydrothermal chimneys. The influence of these microbial metabolisms is evident in shallow subseafloor mixing zones adjacent to high temperature vents. In comparison to conservative mixing of hot vent fluids with deep seawater, diffuse fluids are lower in H_2 and higher in CH_4 (Von Damm and Lilley, 2004; Wankel et al., 2011). Since the temperatures at which mixing takes place are typically too cool for abiotic methanogenesis, this has often been taken as a clear indication that methanogens are responsible for the consumption of H_2 and production of CH_4 (Wankel et al., 2011). Losses of nutrients and other oxidized constituents (nitrate, phosphate, sulfate) in such settings have also been attributed to microbial uptake (e.g. Bourbonnais et al., 2012). One recent study, however, has shown that hydrogen removal can also occur from diffuse flow fluids at temperatures hotter than the known limits for life (~122 °C; Takai et al., 2008), indicating that the non-conservative behavior of geochemical tracers during subseafloor mixing need not always be indicative of microbial consumption (McDermott et al., 2020).

The geo-diversity of submarine hydrothermal circulation

Axial spreading centers

The vast majority of identified hydrothermal systems are hosted on young (<0.1 Ma) ocean crust formed at spreading centers throughout the globe. Fast and super-fast spreading centers are continuously supplied with new injections of magma, form new oceanic crust at rates of 100–140 mm yr^{-1}, and host mafic hydrothermal systems. Intermediate-spreading ridge axes such as the Juan de Fuca Ridge and Gorda Ridge in the NE Pacific host vent fields with similar compositions as they are also largely associated with mafic rocks. Slow (<60 mm yr^{-1}) and ultra-slow (<20 mm yr^{-1}) spreading centers constitute ~50% of all mid-ocean ridge spreading centers by length (Sinha and Evans, 2004), and host more heterogenous vent fields with substantial contributions of ultramafic rocks (Charlou et al., 2010).

To a first approximation, fast spreading ridges are all located in the Pacific Ocean – most notably along the East Pacific Rise which, below 15°S, represents the fastest known spreading center worldwide (Fig. 7). The Mid-Atlantic ridge is slow spreading along its entire length although that spreading rate does also show a further systemic decrease from south to north. Ultraslow spreading centers are found primarily in the Arctic (including the Gakkel Ridge and the Knipovich Ridge which continues south into the Norwegian-Greenland Sea) and the Southwest Indian Ridge which extends from the Rodriguez Triple Junction in the Indian Ocean at its northeast limit, past the southern tip of Africa and into the southernmost Atlantic Ocean at its SW end. The Mid-Cayman Rise represents a much shorter (~100 km), but also much more accessible, segment of ultraslow spreading mid-ocean ridge in the Caribbean Sea.

Mafic dominated venting

Hydrothermal systems hosted in hot, mafic crust are characterized by high temperature fluids that can reach higher than 400 °C in the subsurface (Campbell et al., 1988). Hot, acidic fluids carry high concentrations (μM to mM) of dissolved metals that precipitate upon mixing with cold seawater. Examples of fast and super-fast spreading centers that host hydrothermal fields include the East Pacific Rise as well as the Galapagos Spreading Center, Gorda Ridge, and Juan de Fuca Ridge. Despite its slow spreading rate, mafic dominated vent fields still constitute approximately half of all known vent fields along the Mid-Atlantic Ridge, including the first sites of venting that were found on that ridge at the TAG and Snakepit sites (German et al., 2016a).

Most high-temperature vent fluids have pH values of 3.3 ± 0.5 when measured at 25 °C (German and Von Damm, 2004; see Diehl and Bach, 2020, 2021 for a current global database). Note, however, that the concentration of free H^+ at room temperature differs substantially to that at in situ conditions due to the precipitation of metal sulfides and oxides and dissociation of H^+ and OH^- bearing ion pairs and complexes during cooling (Ding and Seyfried, 2007). As a result, the pH of black smoker fluids is only slightly acidic (5.1–5.4) at in situ conditions (Ding et al., 2005).

The concentrations of volatiles such as CH_4 are generally low in axial mafic hydrothermal systems compared to sedimented or ultramafic systems, though higher than deep seawater (0.3 μmol L^{-1}). Vent fluid CH_4 concentrations are <250 μmol L^{-1} in high temperature fluids from mafic high temperature sites on the East Pacific Rise, Juan de Fuca Ridge, and Mid-Atlantic Ridge (Lang et al., 2019). Concentrations of H_2 are controlled by pressure, temperature, and fluid-mineral equilibria (Seyfried and Ding, 1995). Mineral assemblages that create more reducing redox buffers will lead to fluids with higher concentrations that typically remain <1 mmol L^{-1} H_2, although the very deep and hot Piccard field represents an important exception to that general rule, with concentrations reaching 20 mmol L^{-1} (McDermott et al., 2018). The speciation of sulfur is similarly controlled by interactions with mineral assemblages, leading to millimolar concentrations of H_2S. Both H_2S and H_2 concentrations can spike as a result of magmatic outgassing and lava-seawater reactions after a dike injection or volcanic eruption (e.g. Lilley et al., 2003; Seewald et al., 2003).

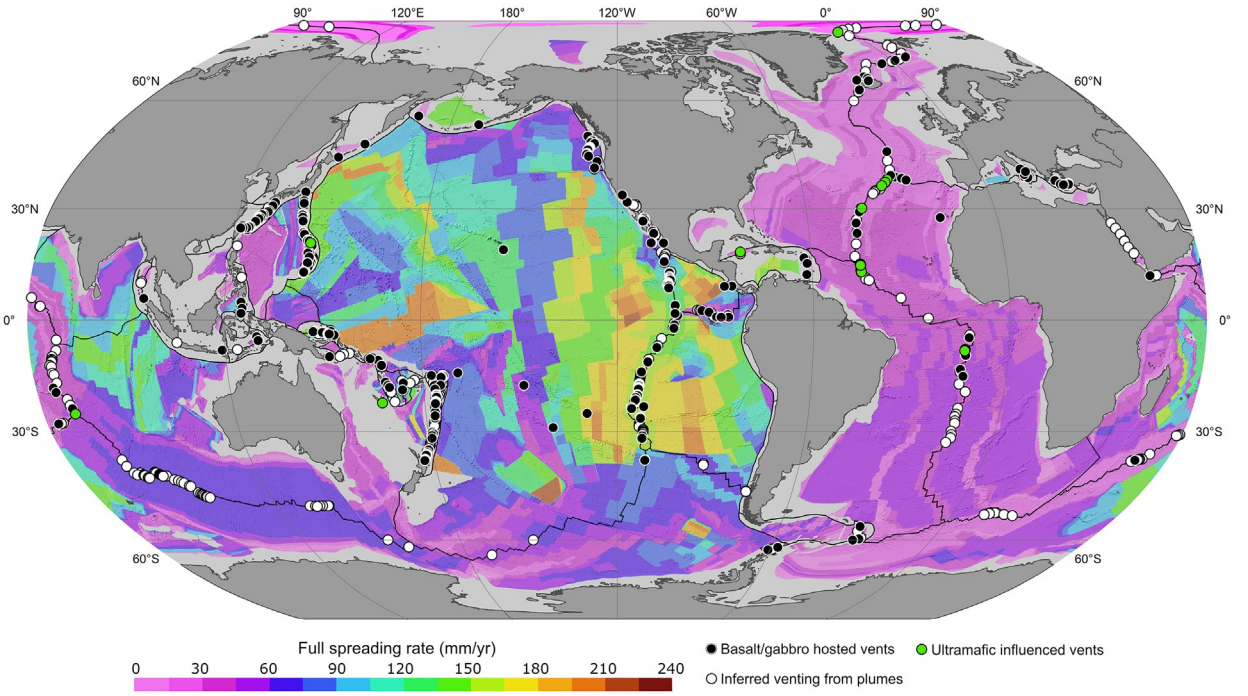

Fig. 7 Map of the half spreading-rate of the oceanic crust (data from Seton et al., 2020) with the distribution of active hydrothermal vents that have been confirmed (colored circles) or are known to exist from the detection of chemical signals in the overlying water column (white circles). Vents with an ultramafic influence are denoted in green and are found along slow- and ultra-slow spreading ridges and in association with subduction zones (<60 mm yr^{-1}). Vent distributions from Beaulieu and Szafranski, 2020. Figure courtesy of Isaac Keohane, U. South Carolina, with input from Stace Beaulieu, WHOI.

Ultramafic influenced venting

Slow and ultraslow spreading centers have less magmatic input and instead are largely tectonically driven (Dick et al., 2003; Snow and Edmonds, 2007). As plates spread, mantle rocks are exhumed from depth and emplaced at the seafloor, exposing ultramafic mantle rocks to seawater (Snow and Edmonds, 2007). In the most extreme cases, systems lack magmatic contributions altogether and fluids are heated by lithospheric cooling alone (Titarenko and McCaig, 2016; Lowell, 2017). Fluid pathways are less channelized than in magmatically-driven systems, leading to the export of hydrothermal fluids across a wide geographical area (Lang et al., 2021). Reactions between seawater and ultramafic rocks result in fluids with distinct geochemical signatures including milli-molar concentrations of H_2 and CH_4, and alkaline pHs (see "Inorganic geochemistry" section, above).

Many systems have both mafic and ultramafic contributions. The Rainbow field (36°N, Mid-Atlantic Ridge) has the high temperature (360 °C), metal-rich (especially high Cu, Fe, and Fe/H_2S), acidic fluids characteristic of a mafic system but also the extremely high H_2 concentrations (16 mM) indicative of ultramafic influence (Charlou et al., 2010). In December 2000, geologists diving at an oceanic core complex at 30°N on the Mid-Atlantic Ridge encountered an entirely new class of lower temperature submarine venting at a field with large (up to 20 m tall) chimneys of calcite [$CaCO_3$], aragonite [$CaCO_3$], and brucite [$Mg(OH)_2$] (Kelley et al., 2005). The Lost City field (30°N, Mid-Atlantic Ridge) exhibits minimal mafic influence and, instead, is dominated by ultramafic characteristics, with maximum temperatures of 115 °C, pH values as high as 11, and H_2 concentrations of 15 mM (Kelley et al., 2005; Proskurowski et al., 2008; Seyfried et al., 2015). In 2010, a more targeted exploration of a similar geologic setting on the Mid-Cayman Rise led to the discovery of ~100–226 °C fluids at the Von Damm hydrothermal field, a truly mixed system with pH values of ~6 to accompany its high H_2 (18 mM) concentrations (McDermott et al., 2015). More recently still, dives to the amagmatic section of the SW Indian Ridge discovered the Old City vent-site that, at least superficially, seems very similar to the Lost City site on the Mid-Atlantic Ridge (Lecouevre et al., 2020).

On-axis diffuse flow

Adjacent to high temperature systems, cold seawater enters the subseafloor and mixes with ascending hot hydrothermal fluids to create lower temperature 'diffuse vents.' Shallow convection through the seafloor also forms low temperature fluids without mixing, as the result of water-rock reactions that alter fluid geochemistry to a lesser extent than in high temperature fluids. The lower temperatures and availability of thermodynamic energy make these particularly favorable locations for the growth of microorganisms and macrofauna. Approximately 50–90% of axial hydrothermal heat flux is thought to be lost via low temperature diffuse venting (Elderfield and Schultz, 1996; Bemis et al., 2012). The degree to which diffuse fluxes impact elemental exports remains very poorly constrained, especially since the mixing geometry of this subseafloor plumbing is thought to vary widely (Lowell et al., 2015). Any non-conservative mixing in the subseafloor will alter these fluxes in ways that are starting to prove important. For

example, dissolved iron, copper, and chromium are stabilized by binding with organic ligands in diffuse fluids, with major implications for the transport of trace metals across ocean basins (Bennett et al., 2008; Sander and Koschinsky, 2011; Lough et al., 2019). Better characterization of the role of diffuse fluids in elemental export and biogeochemical cycling is an important focus of future work (see Section "The biogeochemical significance of low-temperature axial venting", below).

Ridge-flank circulation

As oceanic crust spreads away from the ridge crest it continues to be cooled by advective fluid flow to an age of approximately 65 Ma (Fig. 1); (Stein and Stein, 1994; Johnson and Pruis, 2003). Low-permeability sediment cover slows the exchange of fluid between the ocean and lithosphere, so bare-rock seamounts and other topographic highs are the primary locations of fluid recharge and discharge (Hutnak et al., 2008; Lauer et al., 2018). Regions buried with thick sediments, such as the Juan de Fuca Ridge flank, preclude rapid cooling, causing moderately heated fluids (65 °C) and significant water-rock exchange (Elderfield et al., 1999). However, the vast majority of ridge flank fluids pass through much cooler systems that retain geochemical signatures that are essentially indistinguishable from seawater - as observed, for example, at the Dorado Outcrop (10–20 °C) on 23 Ma crust on the eastern flank of the East Pacific Rise (Mottl and Wheat, 1994; Wheat et al., 2017). Similar crustal aquifers have been accessed directly through drilling in the North Pond sedimented basin on the western flank of the Mid-Atlantic Ridge (Wheat et al., 2020a). Most recently, a large and high temperature hydrothermal vent field has been discovered 750 m east of the ridge-axis on the East Pacific Rise (McDermott et al., 2022), highlighting that there is maybe an even greater variety of off-axis hydrothermal circulation than previously anticipated or, hence, looked for.

Sedimentary inputs

Interactions with sediments can also alter hydrothermal fluid geochemistry. In highly sedimented ridge-flank settings, the base of the sediment layer exchanges with the crustal aquifer, leading to changes in concentrations of Mn, Fe, Mo, Si, PO_4^{3-}, V, and U (Wheat et al., 2013). In extreme cases, mid-ocean ridges abut continental margins sufficiently closely that even the ridge-axis (and associated hydrothermal venting) can become covered in sediments. Where such sediments are primarily biogenic, as found at the Guaymas Basin (Von Damm et al., 1985b) photosynthetically-derived organic matter is decomposed thermogenically to species readily soluble in circulating fluids including NH_4, CH_4, CO_2, Si, and small organic molecules (Von Damm et al., 1985b; Lilley et al., 1993; Cruse and Seewald, 2006).

At higher latitudes, such as at the Escanaba Trough (Gorda Ridge) and Middle Valley (Juan de Fuca Ridge) in the north east Pacific, a slightly different pattern emerges. Vent fluids may continue to emit high concentrations of some dissolved gas species (e.g. $^3He/^4He$, CH_4) but dissolved H_2S concentrations and dissolved metal concentrations tend to be low due to cooling of the fluids as they ascend up through the porous medium of the terrigenous sediment covering the ridge-axis (Campbell et al., 1994; Von Damm et al., 2005). Associated sediments in both the Escanaba Trough and Middle Valley have been found to be enriched in these same metals providing new insights into processes by which metal-rich ore deposits may be generated on land (German et al., 1995; Zierenberg et al., 1998). Evidence for similar sediment-hosted venting has been detected in the past decade at the Chile Triple Junction in the South East Pacific Ocean (German et al., 2022b).

In addition to the settings described above, where sediments overlie the ridge axis, there are also notable sites where sediment is absent from the ridge axis and yet vent-fluid chemistry (notably, enrichments in NH_4^+) appear to reveal compelling evidence for the assimilation of a sedimentary component into water-rock interactions in the subseafloor hydrothermal convection cell. Such signatures have long been recognized at the Endeavour Segment of the Juan de Fuca Ridge (Lilley et al., 1993) but have now also been recognized at the Loki's Castle site on the Mohns Ridge in the Norwegian-Greenland Sea (Baumberger et al., 2016).

Volcanic arcs at convergent plate boundaries

Volcanic arcs are the surface expression of magmatic systems that result from the subduction of mostly oceanic lithosphere at convergent plate boundaries. Submarine volcanic arcs in which both plates are oceanic occur mostly in the western Pacific Ocean, including the Izu-Bonin-Mariana, Tonga-Kermadec, New Hebrides and Aleutian arcs. A notable exception is a short chain in the southern Atlantic Ocean near Antarctica: the South Sandwich arc (German et al., 2000; James et al., 2014). Extensive hydrothermal circulation is associated with both arc and back-arc regions. The Lau Basin and Kermadec Arcs in the southwest Pacific and the Mariana Arc in the western Pacific each host 30–50 volcanos, of which dozens are hydrothermally active (Resing et al., 2009; Baker et al., 2019; Kleint et al., 2019). The magmas formed in arc systems are enriched in volatiles by an order of magnitude compared to MORB (Wallace, 2005; Plank et al., 2013). As a result, fluids tend to be volatile-rich, particularly in CO_2, acidic due in part to magmatic SO_2 degassing, and have high trace metal concentrations (de Ronde and Stucker, 2015). But the wide variety of rock types, the contributions from subducting sediments, the potential for actively erupting volcanoes, and the intersection with other geological processes such as rifting create highly heterogenous fluids and occasional extreme conditions such as the presence of liquid CO_2 or liquid sulfur at the seafloor (Lupton et al., 2006; de Ronde et al., 2015).

Actively erupting volcanoes have been sampled in some back-arc systems, including the West Mata volcano in the Lau Basin (Resing et al., 2011; Baumberger et al., 2014) and NW Rota-1 on the Mariana Arc (Butterfield et al., 2011). Associated fluids contain elevated concentrations of H_2, only slight enrichments of CH_4, and exhibit extremely low pH values of <1.5, all arising from

reactions between molten rock and seawater (Butterfield et al., 2011; Resing et al., 2011). At both West Mata and NW Rota-1, fluids associated with erupting sites did not exit the seafloor via well defined orifices, as is typically observed in ridge-crest systems. Instead, they were found to be pervasive throughout the water column immediately overlying the lava flows, and/or accumulated within any calderas present.

Hydrothermal fluids are also now known to circulate through the forearc regions of subduction zones, such as the Mariana Trench (Fryer, 2012). As the subducting slab loses water, serpentinization of overlying mantle rocks can occur, forming mud volcanoes composed largely of serpentinite grains. The low-chlorinity springs change in composition with distance to the subduction zone, but generally are highly alkaline (pH $>$ 10.7), enriched in dissolved carbonate, CH_4, NH_3, K, Rb, B, and short-chain organic acids (Mottl, 1992; Mottl et al., 2022; Haggerty and Fisher, 1992; Eickenbusch et al., 2019; Wheat et al., 2020b).

Intra-plate hotspots

Volcanoes created by intraplate hotspots occur most prominently in the central and western Pacific Ocean (Galapagos, Hawai'i, Pitcairn, Society Islands, Samoa) and every site that has been investigated to date hosts seafloor hydrothermal activity. They are all relatively low temperature ($<$50 °C) systems, including Galapagos (Corliss et al., 1979), Teahitia (Michard et al., 1993), Kama'e-huakanaloa (formerly Lōihi) (Glazer and Rouxel, 2009), and Vailulu'u (Staudigel et al., 2006). While volcanic activity can lead to transient increases in temperature at the seafloor (Wheat et al., 2000), the emerging general case seems to be that hydrothermal circulation through these tall conical seamounts involves quite distinct subseafloor fluid trajectories. At mid-ocean ridges, down-flow and up-flow limbs of a hydrothermal convection cell occur at very similar depths, along-axis from one another (Fig. 6). In the case of tall, conical intra-plate seamounts, by contrast, recharge occurs close to the base of the seamount, thousands of meters deeper than their summit vents, followed by a long tortuous up-flow stage (Milesi et al., 2023; Chan et al., 2023). This leads to low-temperature fluids discharged from these seamounts, enriched in Fe, Mn, and Si. Despite the low temperature nature of seafloor venting at these intra-plate hot-spots, their fluxes are sufficient to rise significant heights above the seafloor and form non-buoyant hydrothermal plumes (Bennett et al., 2011; German et al., 2020) that can be traced long distances through the oceans (Jenkins et al., 2020).

Transform faults

With the discovery of tectonically-controlled venting at slow, and especially ultra-slow spreading ridges (see Section "Ultramafic influenced venting", above) attention has turned, in the past decade, to ocean transform faults: the third style of active tectonic plate boundary and one that had previously been overlooked. The rationale for such interest is that geothermal gradients exist everywhere in Earth's subsurface and so, logically, deep-penetrating faults that pierce through oceanic lithosphere at transform faults could facilitate pathways for fluid flow, hence, the potential for some form of water-rock geochemical reactions. Systematic exploration of transform faults remains in its infancy (Boettcher et al., 2023) but after nearly 50 years of seafloor exploration for venting, we now recognize that concentrically-zoned metal sulfide deposits dredged from the Romanche Transform (Bonatti et al., 1976) may have represented collection of high temperature chimney material, years before mid-ocean ridge black smoker vents were first discovered.

Hydrothermal interactions with the oceanic water column

In earlier sections, we have described controls on *gross* chemical fluxes to the ocean, based on hydrothermal vent fluid compositions generated from water-rock interactions across a variety of geotectonic settings. These fluxes can increase the concentration of a chemical species in the ocean, such as for vent fluid-enriched metals like lithium (Edmond et al., 1979), or decrease them, such as for vent fluid-depleted ions like Mg (Figs. 5 and 6). However, *gross* chemical fluxes are calculated based on pure endmember fluids exiting the seafloor, and do not always accurately predict the final impact on ocean geochemistry. Further modifications occur when heated vent fluids mix with the cold, oxygenated seawater of the deep ocean in hydrothermal plumes. Geochemical processes in this mixing zone such as precipitation, dissolution, and scavenging can substantially alter *net* hydrothermal fluxes to/from the ocean. Moreover, it is becoming increasingly apparent that many of these processes can be *bio*geochemical. Hydrothermal plumes are important niches for microbiological activity that can impact geochemical fluxes (Dick et al., 2013) and also act as critical dispersal agents for vent-fauna larvae (Adams et al., 2012).

Dynamics of hydrothermal plumes

Hydrothermal plumes are defined as the area encompassing the full mixing gradient between pure juvenile vent fluid and pure ambient seawater. The term "plume" was introduced by Turner (1973) to refer to a feature produced by continuous or steady-state release of a buoyant fluid. The quantitative dynamics of submarine hydrothermal plumes are summarized in Lupton (1995).

There are two main parts of a hydrothermal plume: the buoyant plume and the neutrally-buoyant (or non-buoyant) plume (Fig. 8). As heated vent fluid meets seawater, shear flow at the boundary produces vortices that entrain, or engulf, ambient seawater and mix it with the fluid. This turbulent mixing dilutes the source fluids progressively as the plume rises and facilitates reactions

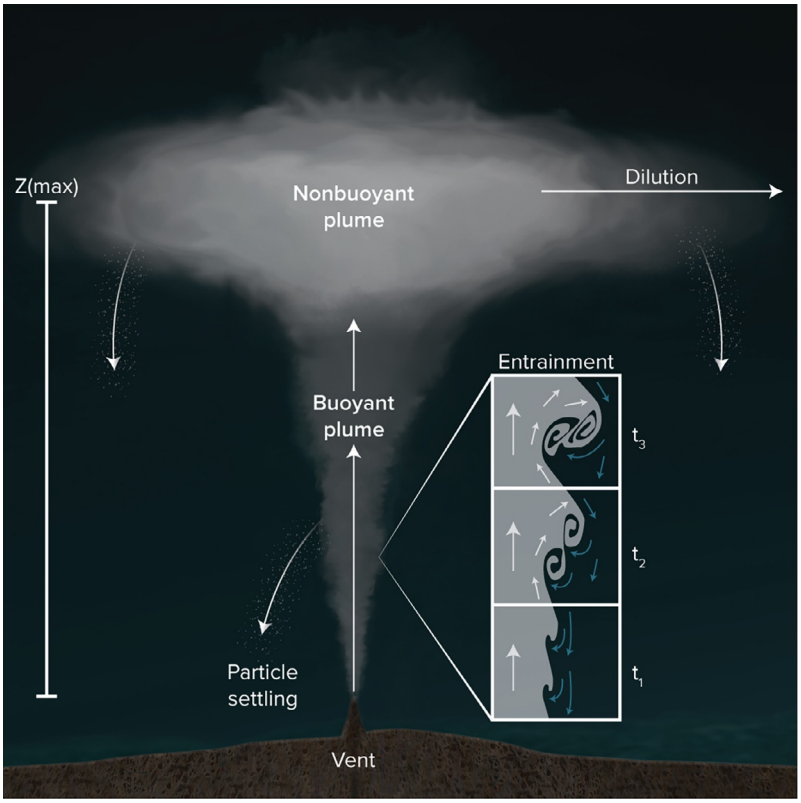

Fig. 8 Sketch of the key physical processes occurring within a hydrothermal plume including entrainment of ambient seawater into the buoyant plume (inset, where t_n indicates increasing time since initiation of vent fluid efflux), rise to a non-buoyant plume height of z_{max} and particle settling from both buoyant and non-buoyant plumes.

between the vent fluids' chemical constituents and the evolving seawater as they continue to mix. Plume mixing vortices are readily visible in the particle-rich columns rising above black smoker hydrothermal vents (Fig. 3).

As it continues to rise, the entrainment of seawater causes the plume to become progressively less buoyant. Eventually, the density of the buoyant plume becomes equal to that of the ambient seawater and, notwithstanding a local effect known as momentum overshoot, the plume ceases to rise. Once it reaches its maximum rise height (z_{max}), the hydrothermal plume begins to spreads laterally as a neutrally buoyant plume (Fig. 8). The value of z_{max} is dependent on the initial buoyancy of the vent fluid, which is primarily a function of the temperature of the vent fluid (hotter fluids are more buoyant), as well as the density stratification of the oceanic water column into which it is injected. Typical z_{max} rise heights for black smoker hydrothermal plumes are 100–400 m above the vent orifice, with the exception of event plumes, which are massive, short-lived plumes that rise up to 1000 m above the seafloor, reflecting transient heat fluxes up to 16 times higher than typical vents (Baker et al., 1989).

The rise velocity of the plume is also related to the density gradient of the ambient seawater, but shows less variability worldwide: the typical rise time to neutral buoyancy is <1 h. The plume is diluted 100–1000-fold in the first 5–10 m of plume rise, and by the time it reaches neutral buoyancy (z_{max}), it has been diluted $\geq$10,000-fold (Lupton, 1995).

Once the neutrally buoyant plume begins to spread laterally, its transport is dominated by the local ocean circulation at plume height. Stommel (1982) famously showed that the geothermal heat carried in the neutrally buoyant plume from the southern East Pacific Rise causes it to expand several thousand kilometers westward, rather than to the south and east as had been predicted by numerical models of deep South Pacific circulation at the time. This is also true on more proximal scales. Within deep axial rift-valleys on slow and ultra-slow ridges, plumes can be subject to topographic steering (German et al., 1998), while even in situations where plumes rise above the height of confining topography, as happens on faster spreading ridges, advanced numerical models require knowledge of not just plume temperature (heat content) but also prevailing deep-ocean currents and the region's high-resolution bathymetry to predict the full complexity of hydrothermal plume transport (e.g. Xu and Lavelle, 2017; Xu and German, 2023). Even surface mesoscale eddies have been shown to have an influence on deep ocean hydrothermal plume transport velocities (Adams et al., 2011), providing further confirmation that the distal transport of neutrally buoyant plumes can be spatio-temporally complex and, hence, challenging to predict.

Biogeochemical processes in hydrothermal plumes

There have been significant efforts to advance our understanding of the geochemistry of hydrothermal plumes during the last decade, with the ultimate goal of quantifying the net flux of elements from hydrothermal vents to the ocean. Principal questions

have included: For which elements are hydrothermal fluids a dominant source to, or sink from, the oceanic inventory? How are elemental fluxes modified by non-conservative chemical and/or biological reactions? What is the impact of hydrothermal processes on the global marine carbon cycle? Here, we address these questions directly by first describing how plumes have been traced into the ocean, then identifying the abiotic solid precipitation reactions that drive the primary non-conservative chemical reactions in hydrothermal plumes (and the associated scavenging effects of other elements onto those particles), and finally addressing the linkages between hydrothermal processes and the global marine carbon cycle.

Tracing hydrothermal plumes

The first challenge of studying hydrothermal plumes is to find and track them, since outside of the immediate area of black smokers, hydrothermal plumes cannot be observed visually. An ideal plume tracer should: (1) behave conservatively (only responding to mixing/dilution, not chemical/biotic reactions), (2) be easy to measure, ideally in real time such as with an in situ sensor, and (3) have a hydrothermal signal that is orders of magnitude higher than its signal in background seawater so that it can be tracked far from the vent site amidst plume dilution. Early plume tracking efforts used sensors either mounted on vehicles or on shipboard CTD rosettes in a grid or tow-yo formation to search for anomalies in temperature and particle-detecting optical signals (transmissometers and backscatter sensors; Lupton, 1995). Sensors detecting changes in seawater oxidation-reduction potential have also been used to detect plumes (Walker et al., 2007), and hydrothermal salinity anomalies have even been detected from Argo floats in some instances (e.g., Guieu et al., 2018). However, most sensors detect plumes only relatively close to sources of vent, because their signals cannot be distinguished from background at factors far beyond $\sim 10^2$–10^4 fold dilution with ambient seawater.

Chemical tracers have the advantage of larger gradients between hydrothermal fluids and seawater, making them more sensitive in distal dilute plumes. However, their disadvantage is that they cannot be measured in real time. The most unambiguous chemical tracer of hydrothermal plumes is helium-3 (^{3}He) because primordial helium was trapped within the Earth's interior at an early stage of planetary formation and has only slowly been released to the deep ocean ever since, through magmatic processes. In the atmosphere, ^{3}He is sufficiently low in mass that it can be lost to space unlike its heavier isotope (formed primarily from alpha-radiation) ^{4}He. Thus, mantle helium is much more concentrated in ^{3}He than oceanic and atmospheric helium, making ^{3}He an extremely sensitive tracer of hydrothermal sources and plumes. One of the original and most famous examples of using ^{3}He to track hydrothermal plumes occurred in the South Pacific, where a ^{3}He plume was observed to disperse >2000 km to the west of the southern East Pacific Rise (Lupton and Craig, 1981). Since then, ^{3}He has been used to trace hydrothermal plumes across numerous ocean basins (e.g. Lupton, 1998), and within the past decade a global database of helium isotope ratios has been published (Jenkins et al., 2019).

As a noble gas, helium behaves conservatively in the ocean, making it even more of an ideal *conservative* plume tracer. This means, it can not only be used to identify plumes but also to normalize other elements to, to account for non-conservative behavior within coherent hydrothermal plumes. For example, normalization to ^{3}He has been used to determine the presence or absence of conservative metal behavior in distal hydrothermal plumes (see Section "Biogeochemical linkages between hydrothermal processes and the marine carbon cycle" below). It must be noted that the pseudo-conservative behavior of dissolved Mn over short time- and length-scales in some hydrothermal plumes has allowed that to be used as a quasi-conservative tracer under certain conditions as well (Field and Sherrell, 2000; Lough et al., 2023), but the long-term non-conservative behavior of hydrothermal Mn limits this approach (Gartman and Findlay, 2020). Radioactive isotopes of both conservative and non-conservative plume tracers, such as ^{222}Rn (Kadko et al., 1990; Rudnicki and Elderfield, 1992), ^{227}Ac (Kipp et al., 2015), and radium isotopes (Kipp et al., 2018; Neuholz et al., 2020) have all been used to calculate ages at different points within hydrothermal plumes. Of these, radium isotopes have recently been shown to be particularly useful in differentiating between the chemical influences of diffuse flow and higher-temperature focused venting (Neuholz et al., 2020).

Iron and manganese precipitation reactions in hydrothermal plumes

Even before hydrothermal vents were discovered, it was known from studies of altered basalts (Humphris and Thompson, 1978) and experiments mixing seawater with basalt at high temperature and pressure (Mottl et al., 1979) that chemically reduced species such as Fe(II), Mn(II), and sulfide should be highly enriched in mafic-hosted hydrothermal fluids. Those early studies found that at the high temperatures of subseafloor venting (200–500 °C), Fe(II) and Mn(II) are released from basalt into aqueous hydrothermal fluids: a flux stabilized by the low pH resulting from H^+ release during the subseafloor transformation of seawater Mg^{2+} into secondary alteration minerals. The presence of ferrous Fe(II) in vent fluids is especially important because it quickly consumes dissolved oxygen, leaving vent fluids anoxic. Additionally, Fe(II) reduces seawater sulfate into sulfide, adding to the high temperature mafic sulfide flux that is otherwise limited to the concentrations of sulfate in downwelling water feeding the host hydrothermal system. Indeed, dissolved Fe, Mn, and sulfide are some of the most concentrated species in high-temperature hydrothermal fluids, and their vent fluid concentrations (mM) can be enriched by more than a million times over their open ocean concentrations (sub nM).

The abundance of these reduced Fe, Mn, and S species in hydrothermal fluids is important because, once they meet the low temperatures and oxidizing conditions of seawater, they spontaneously and abiotically precipitate solids that build hydrothermal chimney structures and turn the discharging fluid black.. Chemically, Fe(II) is highly soluble in the absence of oxygen, especially at low pH, while its oxidized counterpart Fe(III) is most stable as oxidized Fe(III) oxyhydroxide solids in oxic seawater (Millero et al., 1987). Similarly, abiotic sulfide oxidation by oxygen and its radicals is kinetically favorable, especially in the presence of Fe or Mn oxides (Luther et al., 2011).

Thus, when reducing vent fluids mix with ambient seawater in a buoyant hydrothermal plume, a two-step non-conservative reaction series is initiated that results in an abundance of solid precipitates (Mottl and McConachy, 1990). First, the instantaneous cooling of the vent fluid from >300 °C to ≤30 °C results in the precipitation of a range of Fe sulfides (note that Mn does not readily precipitate sulfide minerals). Though hydrothermal chimney formation is initiated by anhydrite formation when seawater sulfate meets the high temperature fluids (Haymon, 1983), the metal sulfide solids formed from vent-fluid quenching eventually replace the anhydrite, resulting in the canonical sulfide-rich chimney structures of hydrothermal vents with concentric outer layers of Fe/Cu/Zn sulfides including pyrite, chalcopyrite, sphalerite, and pyrrhotite. These non-conservative Fe—S precipitation reactions can occur sub-seafloor, if cold seawater is entrained locally, or above the seafloor within the buoyant hydrothermal plume once fluids exit the seafloor.

The second step of the principal non-conservative buoyant plume reactions occurs when entrainment of oxic seawater initiates redox reactions that rapidly oxidize Fe(II) to Fe(III), as well as sulfide to a range of intermediate mixed sulfur products including sulfate. Then, the low solubility of the oxidized Fe(III)(aq) following Fe(II) oxidation (Millero, 1998) initiates the precipitation of Fe oxyhydroxide solids that can also dominate the plume. The vent fluid's Fe:S ratio can be used as a guide for how much Fe—S precipitate can form prior to Fe(II) oxidation (Gartman et al., 2014; Gartman and Findlay, 2020), though it is not the only control on the balance of Fe—S vs. Fe oxyhydroxide precipitates, as sulfide undergoes its own oxidation reaction series independent from Fe (Mottl and McConachy, 1990). Iron isotope studies of hydrothermal systems, especially those combined with sulfur isotopes, have proven very useful in constraining the extent of Fe precipitation with sulfides above and below the seafloor (Severmann et al., 2004; Rouxel et al., 2008).

Once the Fe precipitates as a sufficiently large particle, it is removed from the ocean via gravitational settling to form metalliferous sediments (Fig. 2). This is important for two reasons. First, aggregative removal of hydrothermal Fe to the sediments effectively reduces the net flux of dissolved Fe to the oceanic inventory, with biogeochemical implications (see Section "Biogeochemical linkages between hydrothermal processes and the marine carbon cycle" below). Second, settled Fe and Mn particles can also transport a host of other scavenged metals to the underlying sediments (see Section "Hydrothermal plume scavenging" below). As a result, the partitioning of Fe in hydrothermal plumes into dissolved and particulate size fractions is critical for calculating net hydrothermal fluxes for a range of elements; this partitioning is determined in large part by the Fe(II) oxidation rate (Gartman and Findlay, 2020). Field and Sherrell (2000) first predicted that the oxidation rate for Fe(II) in hydrothermal plumes should decrease along the path of oceanic overturning circulation, reflecting the progressively decreasing pH and dissolved oxygen content of older deep waters (Fig. 9). This pattern has borne true with observed Fe(II) half lives of 2–3 min in the North Atlantic Ocean (Rudnicki and Elderfield, 1993) and ~2 h in the older Central Indian Ridge (Statham et al., 2005). However, recent detailed measurements of hydrothermal Fe(II) lifetimes do show some shorter and longer lifetimes than kinetically-predicted, and these have been attributed to the influence of ligand chelation and colloids (González-Santana et al., 2021; Wang et al., 2012). Over the last decade, Fe isotopic measurements of dissolved and particulate Fe in vent fluids and hydrothermal plumes have proven extremely useful for mapping Fe(II) sulfide formation and precipitation, as well as the extent of Fe(II) oxidation and subsequent loss by aggregative precipitation as Fe oxyhydroxides (Rouxel et al., 2008, 2018; Bennett et al., 2009; Klar et al., 2017; Lough et al., 2017; Fitzsimmons and Conway, 2023).

Finally, dissolved Mn(II) is also often enriched over seawater concentrations by $>10^6$ in hydrothermal fluids, but unlike Fe(II) and sulfide its abiotic oxidation by dissolved oxygen is kinetically inhibited (Nealson et al., 1988). Nonetheless, Mn(II) can be oxidized in hydrothermal plumes to form MnO_2(s) and Mn-oxyhydroxide particles either abiotically, via catalytic oxidation accelerated by adsorption onto mineral surfaces, particularly Fe oxyhydroxides (Davies and Morgan, 1989), or through biotic (bacterial) oxidation (Tebo et al., 2004). These Mn oxide solids also serve as elemental scavenging sites (see Section "Hydrothermal plume scavenging" below), though the trajectories of Fe and Mn oxides in hydrothermal plumes are decoupled (Fitzsimmons et al., 2017). Importantly, since the oxidation of Mn(II) occurs in one-electron steps (Luther, 2005), Mn(III) is formed as an intermediate that can be stabilized by organic ligands in solution and has been found to compose up to 64% of the dissolved Mn in hydrothermal plumes (Thibault de Chanvalon et al., 2023).

Hydrothermal plume scavenging

The importance of Fe and Mn precipitation reactions in hydrothermal plumes is due partly to their oxides serving as the dominant chemical "scavengers of the sea" (Goldberg, 1954). Chemical scavenging is defined here as any process that moves elements from the dissolved to the particulate phase, whereupon gravity then removes the particles from the oceanic inventory to underlying sediments. Scavenging in hydrothermal plumes involves four potential processes: (i) co-precipitation, which is the incorporation of other elements into the mineral during the solid precipitation reaction; (ii) adsorption, which is the (sometimes reversible) process whereby elements attach onto the surfaces of particles; (iii) aggregation, which is the agglomeration of many nanoparticles into larger particles of sufficient size to experience gravitational settling; and (iv) biological uptake into cells of particulate size. Importantly, Fe and Mn oxide authigenic particles, formed as described in Section "Iron and manganese precipitation reactions in hydrothermal plumes" above, facilitate significant scavenging of other elements and are considered to have highly reactive surfaces. As a result, the formation, scavenging, and subsequent settling of Fe and Mn (oxyhydr)oxides can have a major impact on the net hydrothermal impact on the oceanic inventories of other elements.

Different elements in seawater have unique reactivities to Fe and/or Mn oxyhydroxides, depending on their chemistry, and thus the distribution of hydrothermal Fe and/or Mn oxyhydroxides formed in plumes has differential effects on the net fluxes of elements to the ocean. The various scavenging behaviors of different elements can be organized into three main categories, based on the

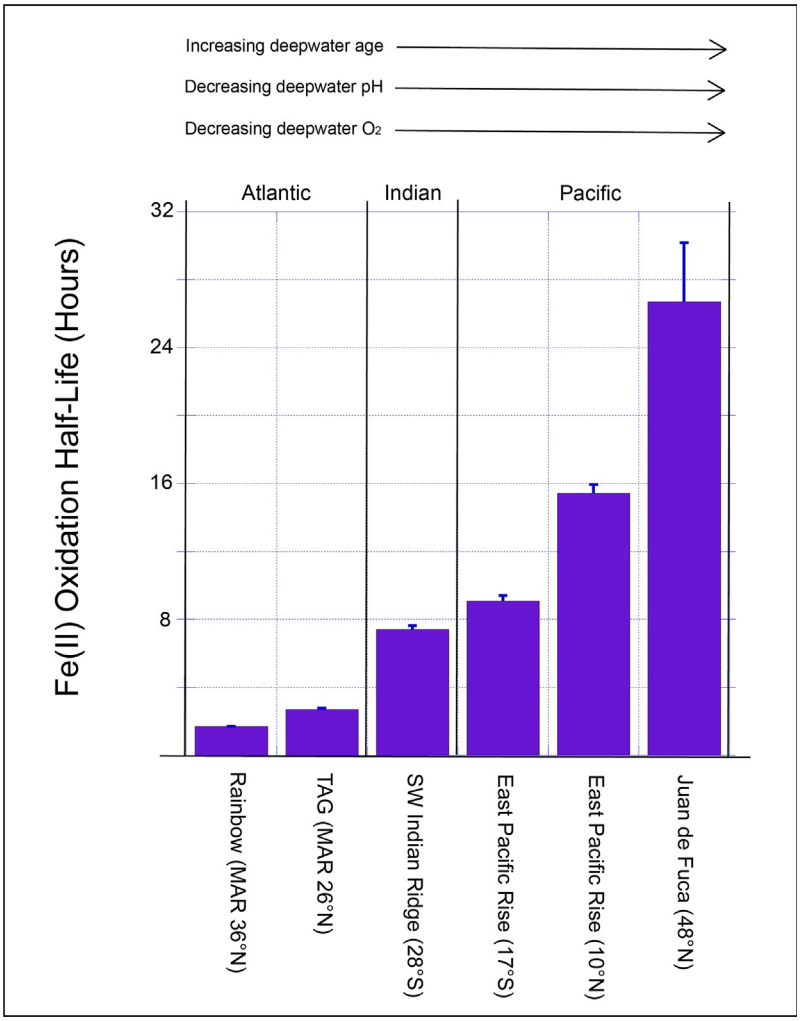

Fig. 9 Fe(II) oxidation half-lives are re-calculated here from Field and Sherrell (2000) at different hydrothermal vent sites across the global ocean, based on Fe(II) oxidation rate laws established by Millero et al. (1987) and updated by Magdalena Santana-Casiano et al. (2005) and González-Santana et al. (2021). Importantly, as deep waters age and accumulate remineralized products from cumulative respiration from the North Atlantic to the North Pacific over meridional overturning circulation, their pH and oxygen concentrations both decrease, which extends the lifetime of Fe(II). Since the extent of Fe(II) oxidation of vent fluid Fe sets an important boundary between "near-field" and "far-field" hydrothermal systems (Gartman and Findlay, 2020), the spatial extent of these redox boundaries would change between vent systems in the North Atlantic and Pacific Oceans.

relationship between their particulate metal concentrations compared to particulate Fe concentrations in hydrothermal plumes (German et al., 1991a). The first group is the "chalcophilic" (sulfur-loving) elements, including copper, zinc, and lead, whose particulate concentrations have a curved downward relationship relative to particulate Fe in plumes (Fig. 10, top). These soft metals co-precipitate with Fe sulfides that form in the buoyant plume and thus are net removed from seawater. Across the open ocean, Boyle et al. (2020) have showed that even though Pb concentrations are extremely high within East Pacific Rise vent fluids, representing a gross source flux to seawater, the removal of Pb by scavenging onto Fe sulfides in the Southern East Pacific Rise hydrothermal plume is so significant that only 1% of the basaltic Pb isotope signature can be identified. Overall, oceanic dissolved Pb is removed to lower-than-background concentrations by scavenging onto ferromanganese hydrothermal particles. In contrast, even though chalcophilic zinc co-precipitates with sulfides and can form sulfide minerals of its own such as sphalerite, the concentration of zinc in hydrothermal plumes can sometimes exceed that of background seawater (Roshan et al., 2016; John et al., 2018), indicating that there is a complex balance of vent fluid sources vs. hydrothermal plume sinks that sets the net flux of chalcophile metals to the ocean inventory.

The second group of hydrothermally scavenged elements are interesting because their particulate concentrations have linear, fixed relationships with particulate Fe in hydrothermal plumes, independent of dilution or distance downstream of the vent site (Fig. 10, center). These elements include phosphorus, vanadium, arsenic, and uranium, all of which form oxyanions in seawater (PO_4^{3-}, VO_4^{3-}, $HAsO_4^{2-}$, and $UO_2(CO_3)_3^{4-}$). These elements are not particularly enriched in hydrothermal fluids, but they are net removed from seawater onto freshly formed, sinking iron oxyhydroxide particles in hydrothermal plumes. A particular example of

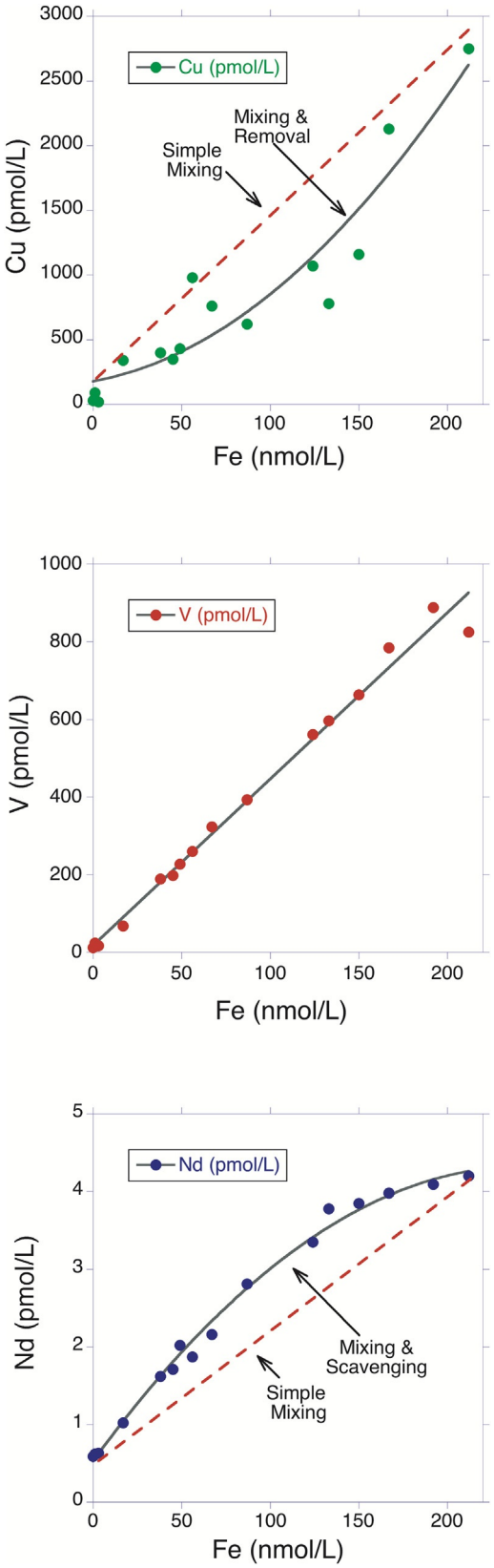

Fig. 10 Three behaviors characterize the scavenging of elements in hydrothermal plumes, identified based on plots of particulate metal concentrations versus particulate Fe for suspended particulate material filtered in situ from the TAG hydrothermal mound, Mid-Atlantic Ridge, 26°N (data replotted from German et al., 1991a). Top: Particulate Cu represents chalcophilic elements that co-precipitate with Fe as sulfide phases and then settle to the seafloor. Middle: Particulate V represents the oxyanions that co-precipitate with Fe oxide phases in hydrothermal plumes. Bottom: Particulate Nd represents surface-reactive elements that adsorb to the surfaces of ferromanganese oxides.

this is the removal of dissolved phosphate from hydrothermal plumes that has been noted for decades (Feely et al., 1990). Additionally, even though vanadium can be enriched in vent fluids, dissolved vanadium is overwhelmingly removed from seawater by coprecipitation into ferromanganese oxyhydroxides in hydrothermal plumes (Trefry and Metz, 1989; German et al., 1991a; Ho et al., 2018).

The third group of elements scavenged from hydrothermal plumes are the particle reactive elements beryllium, thorium, protactinium, and the rare earth elements (REEs), which present upward curved relationships relative to particulate Fe in hydrothermal plumes (Fig. 10, bottom). These elements undergo surface adsorption onto Fe and Mn oxyhydroxide particle surfaces, with the highest metal/Fe ratios observed farthest from the plume, due either to kinetic controls as hydrothermal particles continue to adsorb these metals downstream (German et al., 1990) or thermodynamic control as particulate Fe concentrations decrease downstream (Sherrell et al., 1999). Importantly, based on their points of zero charge (Stumm and Morgan, 1996), amorphous Fe oxyhydroxide surfaces have near neutral or slightly positively charged surfaces, while most Mn oxide minerals have negatively charged surfaces. These surface charges control which elements adsorb to the surfaces of Fe vs. Mn oxide particles, because various elements form either positively or negatively charged aqueous complexes at seawater pH (Byrne, 2002) that are differentially attracted to the positive or negatively charged particle surfaces. The resulting elemental scavenging patterns have been well characterized for ferromanganese crusts (Koschinsky and Hein, 2003), with implications for closely related authigenic Fe and Mn oxyhydroxide particles. This is important because particulate Fe and Mn have been shown to be spatially decoupled in hydrothermal plumes (Fitzsimmons et al., 2017), and thus the scavenging impact on different elements binding to one particle type or the other could become similarly decoupled in space. Dissolved thorium, protactinium, and the REEs have all been shown to be progressively removed from hydrothermal plumes with increasing distance from their vent source (German et al., 1990, 1991a,b; Stichel et al., 2018; Pavia et al., 2018, 2019). In conclusion, regardless of whether subseafloor hydrothermal reactions enrich elements in vent fluids, hydrothermal systems can sometimes act as a net sink of those same elements from the ocean due to scavenging onto authigenic ferromanganese particles in hydrothermal plumes.

Biogeochemical linkages between hydrothermal processes and the marine carbon cycle

We have described, above, how cumulative hydrothermal processes (subseafloor and within hydrothermal plumes) serve to modify net chemical fluxes to the ocean. Accordingly, it is important to understand what impact such cumulative hydrothermal processes might have on the global marine carbon cycle.

The most obvious impact is the potential for a direct, gross flux of organic carbon to or from the ocean. As discussed above, the few high-temperature vent fluids that have been analyzed appropriately have been found to be depleted in dissolved organic carbon (Lang et al., 2006), representing a global sink of refractory dissolved organic compounds (Hawkes et al., 2015; Shah Walter et al., 2018). In contrast, low-temperature diffuse flow fluids are enriched in dissolved organic carbon, associated with elevated microbial biomass in the same fluids (Lang et al., 2006). Indeed, the unique elemental fluxes from vent fluids fuel a vast ecosystem at and beneath the seafloor, and within overlying hydrothermal plumes, via extensive chemosynthetic primary production involving a diverse array of microbes (Huber et al., 2002; Sylvan et al., 2012; Dick et al., 2013; Cohen et al., 2021). In the past decade, it has been estimated that 10–33% of all particulate organic carbon sequestered from the abyssal ocean to the seafloor, worldwide, may have originated in hydrothermal plumes (German et al., 2015), revealing a direct coupling between hydrothermal processes and *deep* ocean organic carbon inventories (Fig. 11).

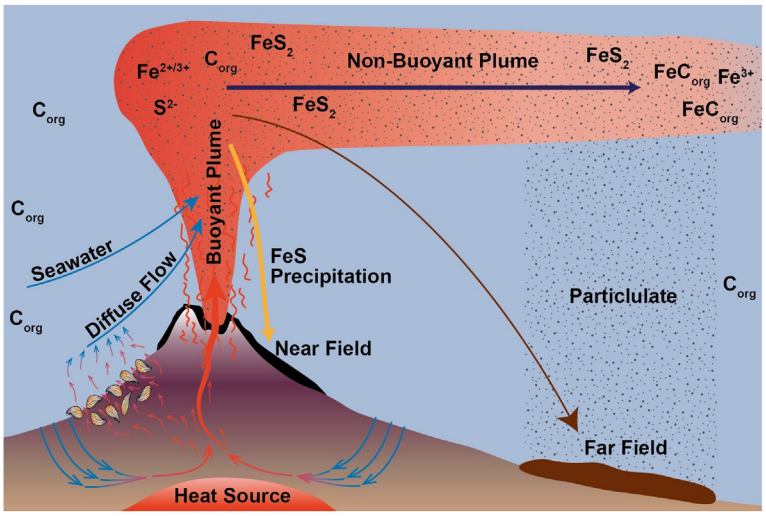

Fig. 11 Schematic of processes associated with three sources of fluids to buoyant hydrothermal plumes: focused vent flow into the buoyant plume, diffuse vent flow (which can be entrained into the buoyant plume), and seawater (which is assumed to be entrained into and dilute the buoyant plume). Extensive precipitation of polymetallic sulfides occurs as the temperature drops and oxygen rises in the buoyant plume, resulting in an important settling flux of metalliferous sediments immediately around the vent orifice. However, Fe and carbon chemistry are linked in the hydrothermal plume. Organic carbon complexes with both dissolved and particulate Fe phases in the hydrothermal plume. Reversible scavenging and settling of metalliferous particles is thus regulated by this organic carbon complexation, while particulate organic carbon from the plume itself also rains out to the sediments beneath hydrothermal plumes. Figure from German et al. (2015).

However, hydrothermal processes may also have an upper ocean impact on the marine carbon cycle via the fertilization of surface ocean photosynthetic primary production. It is well established that photosynthetic organisms carry a high biochemical requirement for the micronutrient Fe (Twining and Baines, 2013; Morel et al., 2014). Due to this high cellular Fe requirement, combined with the low solubility of Fe in seawater (Liu and Millero, 2002), photosynthetic primary production in vast portions of the global surface ocean is limited by insufficient availability of the micronutrient Fe, an idea originally termed the 'Iron Hypothesis' (Martin and Fitzwater, 1988; Martin, 1990). These Fe-limited regions, termed High-Nutrient Low-Chlorophyll (HNLC) zones, include the subarctic and equatorial Pacific and the Southern Ocean and account for up to 40% of the surface ocean's area, according to global biogeochemical models (Moore et al., 2002). Thus, understanding which sources of Fe to the ocean effectively fertilize this photosynthetic primary production is critical to understanding global carbon sequestration on both modern and glacial-interglacial timescales (Tagliabue et al., 2014; Sigman and Boyle, 2000).

Throughout the 1990s as the Iron Hypothesis gained traction, hydrothermally-derived Fe was thought to precipitate quantitatively, effectively removing the entirety of its massive gross flux to metalliferous sediments (German et al., 1991a). As a result, early iron biogeochemical models did not consider hydrothermal vents to be a biogeochemically-significant flux of Fe. However, as new, high-quality dissolved Fe data began to accumulate, after the turn of the millennium, similarities between Fe and ^{3}He profile shapes in far-field hydrothermal plumes introduced the possibility that a fraction of hydrothermal Fe could be stabilized against precipitation to persist as a net source to the oceanic dissolved Fe inventory (Wu et al., 2011; Fitzsimmons et al., 2014). This hypothesis was termed the "Leaky Vent Hypothesis" (Toner et al., 2012). In an influential early study, biogeochemical modeling was used to predict that hydrothermal Fe could supply sufficient dissolved Fe to fertilize photosynthesis in Southern Ocean surface waters, significantly increasing carbon export there compared to non-hydrothermal simulations (Tagliabue et al., 2010). This led to significant interest in hydrothermal processes as a potentially significant and important source flux of bioavailable Fe to the ocean.

The international GEOTRACES Program (SCOR Working Group, 2007), which is focused on identifying the processes and quantifying the fluxes controlling the distributions of trace elements and isotopes throughout Earth's oceans, has made significant strides in understanding the role of hydrothermal Fe in surface ocean fertilization and carbon export. First, the international GEOTRACES sections have provided global evidence that hydrothermal Fe is preserved in the dissolved phase of distally-transported hydrothermal plumes – in the North Atlantic (Fitzsimmons et al., 2015a; Hatta et al., 2015; Lough et al., 2023), South Atlantic (Saito et al., 2013), Pacific (Resing et al., 2015; Fitzsimmons et al., 2017; Jenkins et al., 2020), Arctic (Klunder et al., 2012; Gerringa et al., 2021), Indian (Nishioka et al., 2013), and Southern Oceans (Klunder et al., 2011; Sieber et al., 2021). It has become clear, from these studies, that there is a net export flux of Fe from hydrothermal systems into the deep ocean. The GEOTRACES GP16 transect (Moffett and German, 2018) specifically targeted the >4000 km-long hydrothermal plume emanating from the Southern East Pacific Rise (Resing et al., 2015; Fitzsimmons et al., 2017) and produced the now-canonical images of distal transport of dissolved and particulate Fe and Mn in hydrothermal plumes (Fig. 12).

Two mechanisms have been proposed for how this hydrothermally-sourced Fe may be protected against precipitation and maintained in some dissolved form (Fig. 11). The first is that the Fe *does* precipitate but only at the nanoparticulate scale, which falls within the operationally-defined dissolved size fraction. For example, pyrite nanoparticles are known to form in hydrothermal fluids (Yucel et al., 2011; Gartman et al., 2014; Findlay et al., 2019). Their small size prevents them from sinking, although it is clear from recent electron microscopy imaging that hydrothermal Fe oxyhydroxide nanoparticles do aggregate into larger-sized particles that settle within the plume (Hoffman et al., 2020), perhaps facilitated by entrained organic carbon (Hoffman et al., 2018). The second potential mechanism is that organic ligands chelate the Fe, effectively protecting the Fe against solid precipitation (Bennett et al., 2008; Sander and Koschinsky, 2011). Cathodic stripping voltammetry methods have been used to analyze hydrothermal plume Fe, both in the forward competitive ligand exchange mode (Bennett et al., 2008; Buck et al., 2018) and in the reverse titration mode (Hawkes et al., 2013). While these methods cannot distinguish nanoparticulate minerals from Fe bound to strong organic ligands, an excess of organic ligands is observed in distal hydrothermal plumes, suggesting that at least some hydrothermal organic ligand source must exist, potentially derived from lower-temperature diffuse flow fluids known to produce dissolved organic carbon and/or the microbes associated with hydrothermal plumes (Li et al., 2014).

Thus, current research into the role of hydrothermal Fe in surface ocean carbon sequestration is focused on (1) determining the speciation of dissolved Fe in hydrothermal plumes and (2) predicting or measuring the lifetimes of different dissolved Fe species in seawater against their natural abiotic scavenging lifetimes, which would remove the Fe from the ocean to the sediments. New methods continue to be applied to the first question, including novel siderophore detection methods (Hoffman et al., 2020; Monreal et al., 2021) and Fe isotope approaches that can be modeled to distinguish nanoparticulate from organically-chelated hydrothermal Fe (Steffen et al., 2024). In addition, global biogeochemical Fe models have significantly advanced the residence time question by parameterizing hydrothermal Fe fluxes into Fe biogeochemical models and calculating their impact on carbon sequestration (Resing et al., 2015; Tagliabue and Resing, 2016). These modeling efforts have shown, for example, that although the SEPR flux of dissolved Fe is large (Fig. 12), most of it gets trapped in the deep Pacific Ocean, while only ~1% of it reaches the surface ocean (Roshan et al., 2020). When extrapolated globally, the greatest biogeochemical impact of vent Fe fluxes arises from vents with the shortest transit times to surface waters, including both shallow vents and vents within the Southern Ocean (Tagliabue and Resing, 2016; Roshan et al., 2020). Several recent efforts have shown that shallow hydrothermal and volcanic Fe fluxes can, indeed, stimulate phytoplankton blooms in Fe-limited regions such as the Western Tropical South Pacific and the Southern Ocean (Guieu et al., 2018; Bonnet et al., 2023). There has also been renewed interest in the fate of dissolved Fe from shallow intraplate vents (Fitzsimmons et al., 2015b; German et al., 2020; Jenkins et al., 2020). Finally, recent work has identified five major topographic features in the southern ocean that greatly enhance localized upwelling (Tamsitt et al., 2017). At two of these locations,

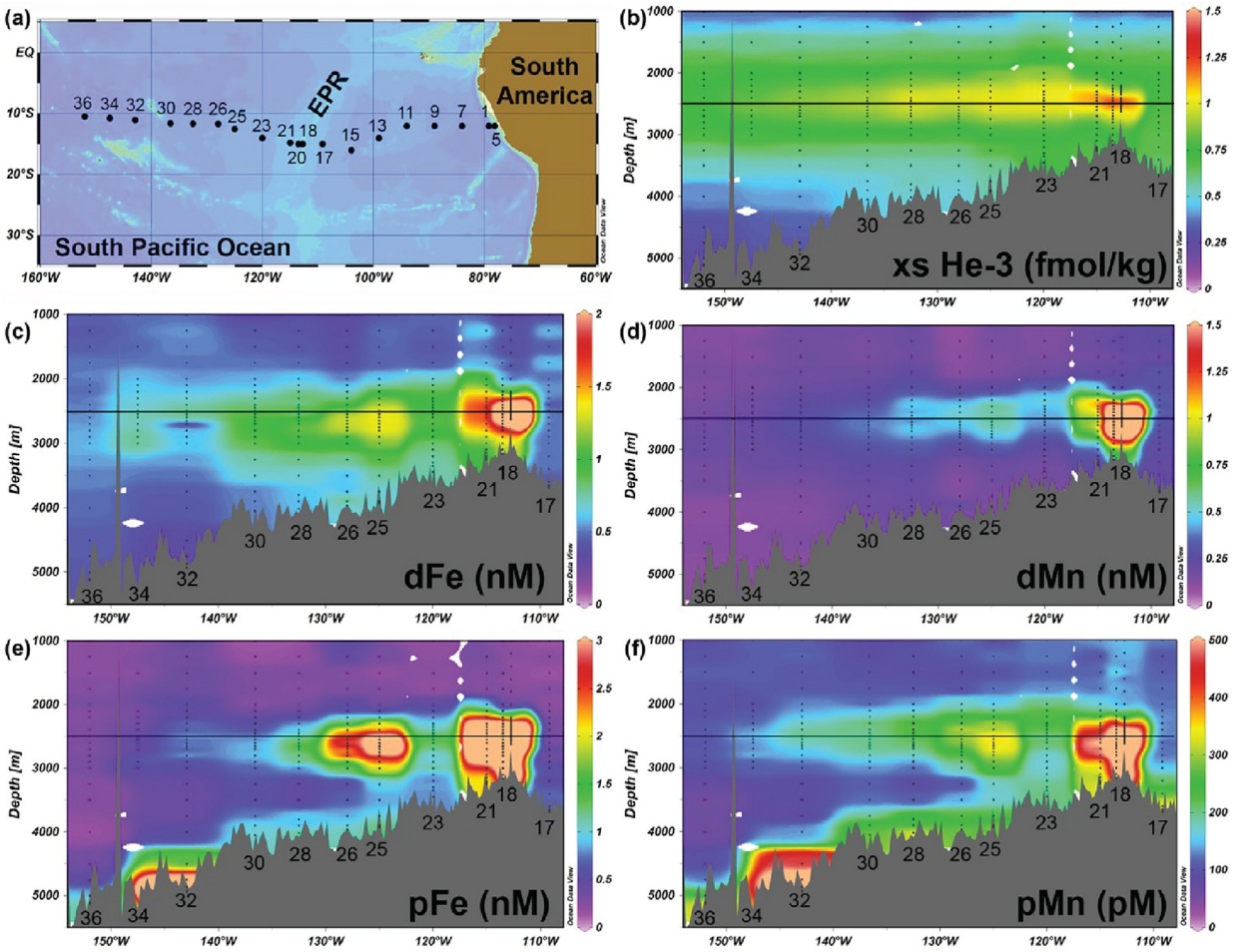

Fig. 12 A major hydrothermal plume sourced close to 15°S on the superfast-spreading East Pacific Rise extends westward for >4000 km across the South Pacific basin (a) to at least 150°W, due north of Tahiti, based on results from the U.S. GEOTRACES GP16 East Pacific Zonal Transect (Resing et al., 2015; Fitzsimmons et al., 2017). This plume was identified based on its excess ^{3}He (xs He-3) concentrations (b), but it also carries dissolved Fe and Mn along its length (c and d), as well as particulate Fe and Mn (e and f). This section has been used to show the critical decoupling of Fe and Mn phases along the plume trajectory due to reversible scavenging of Fe onto sinking particles, with implications for many other trace elements and isotopes that bind onto the surfaces of the hydrothermal ferromanganese oxide particles.

in the Indian Ocean, the associated upwelling has since been recognized to facilitate hydrothermal Fe fertilization of anemic Southern Ocean phytoplankton communities (Ardyna et al., 2019). This places a major focus of future work on Southern Ocean hydrothermal vents, not least along the largely unexplored Pacific-Antarctic Ridge (Beaulieu et al., 2015).

In summary, it is clear that hydrothermal processes have both direct and indirect impacts on the global carbon cycle, although the full extent of these processes remains to be quantified. Modern advancements in interdisciplinary techniques have facilitated a crescendo of both field-based and modeling-based research that have revealed and will likely continue to highlight the impact of these unique biogeochemical systems on oceanic carbon sequestration.

Future research directions

The field of seafloor hydrothermal research continues to yield surprising results at scales that range from individual vent-sites to entire ocean basins and even to other planetary bodies. In this final section we focus on two novel areas of research that we anticipate could prove particularly fruitful in the decade ahead.

The biogeochemical significance of low-temperature axial venting

Implicit in previous editions of the Treatise of Geochemistry, was an assumption that high temperature venting at ridge axes represented the dominant source of hydrothermal chemical fluxes to the oceans (German and Von Damm, 2004; German and Seyfried, 2014). This argument appeared only to be strengthened in the past decade, with the advent of the international

GEOTRACES program. Results from that program allowed us to deduce that (i) hydrothermally sourced trace elements and isotopes (TEIs) are dispersed over long distances in every ocean basin (German et al., 2016b); (ii) enrichments in particulate as well as dissolved TEIs in hydrothermal plumes can be traced across entire ocean basins (Fitzsimmons et al., 2017); and (iii) hydrothermally sourced Fe can persist far enough to be upwelled into HNLC waters to fuel high-latitude primary productivity with a concomitant draw-down of atmospheric CO_2 (Resing et al., 2015; Ardyna et al., 2019; Jenkins et al., 2020). Contemporaneously, a first detailed geochemical study of a cool hydrothermal system (CHS) on an un-sedimented ridge-flank revealed that for many species, CHS fluids exhibit compositions that are largely indistinguishable from their seawater progenitors (Wheat et al., 2017). Thus, while large fluxes of water and heat through ridge-flank circulation may not necessarily impact global-scale budgets, on-axis sources do provide significant export fluxes of trace elements and isotopes to the oceans.

Since the 2nd edition of the Treatise of Geochemistry (German and Seyfried, 2014) was published, however, technological advances in exploration strategies and in situ sensing have led to the realization that low-temperature hydrothermal systems along medium and fast-spreading ridges are far more numerous than high temperature systems (Baker et al., 2016; Chen et al., 2020). To date, however, studies of the biogeochemical significance of these systems remain in their infancy. Further, these phenomena have been identified to date only from surveys in the Pacific Ocean, along medium- to super-fast spreading ridges.

On-axis, low-temperature flow - whether or not it is associated with high temperature fields - might be more important as a source of chemical fluxes to the ocean than has previously been appreciated. Historically, our understanding of low-temperature hydrothermal fluxes associated with black-smoker vents was limited to a few site-specific studies on the Juan de Fuca Ridge, leading to estimates that as much as 90% of fluids heated to ~350 °C during high temperature ridge-axis circulation might exit the seafloor at much lower temperatures after mixing with seawater in the shallow subsurface (Schultz and Elderfield, 1997). Interest in what the *bio*geochemical impact of such flow might be was only renewed by SCOR WG 135 in the past decade, however, in the context of how organic complexation, linked to diffuse flow, might facilitate long-range transport of Fe to the ocean (German et al., 2015). That study compared global-scale estimates of hydrothermal Fe fluxes with what could be constrained from the EPR 9°50′N hydrothermal field and generated a surprising prediction: that ~90% of hydrothermally-sourced Fe dispersed through non-buoyant hydrothermal plumes worldwide may have been sourced from low-temperature on-axis vent-fluxes rather than from black smokers. Subsequently, Baker et al. (2016) and Chen et al. (2020) have used results from dedicated surveys close to the seafloor along mid-ocean ridges to detect evidence of low-temperature flow that is independent of high-temperature venting, using in situ oxidation/reduction probes. When compared to estimates made from conventional "tow-yo" surveys that prospect for particle-rich non-buoyant hydrothermal plumes arising from black smoker activity (Baker et al., 1995), these new studies have revealed that low temperature flow-sites, which emit fluids out of chemical (redox) equilibrium from the overlying water column, may be far more numerous than high-temperature vents. How significant might the biogeochemical *fluxes* from this lower-temperature on-axis flux be?

To address this, we recommend an approach that would seek to determine both the integrated fluxes and the partitioning of those fluxes across an entire vent-field. As discussed in the previous edition of this chapter, a first attempt to evaluate export fluxes from a single vent-site to the oceans at the Rainbow hydrothermal field sought to exploit the dispersion of a non-buoyant hydrothermal plume, restricted within the confines of the rift-valley of the Mid-Atlantic Ridge, in a region of monotonous uni-directional crossflow. In that study, it was assumed that *all* hydrothermal flux of geochemical significance was channeled through neutrally buoyant hydrothermal plumes that were analyzed no more than 5–10 km downstream from their source (German et al., 2010). What we now appreciate, thanks to the advances achieved through the GEOTRACES program, is that such an approach was flawed in two ways. First, the past decade has revealed that important processes that regulate the *net* flux from hydrothermal venting within dispersing non-buoyant plumes may occur over length scales greater than just 5–10 km (perhaps up to 100 km?) downstream from their source (Fitzsimmons et al., 2017). Second, it is no longer a safe assumption that geochemical fluxes from the seafloor – at mid-ocean ridges or in other settings – are dominated by high-temperature hydrothermal venting, nor that all outputs from low-temperature on-axis venting are entrained into neutrally buoyant hydrothermal plumes (Baker et al., 2016; Chen et al., 2020).

For this reason, it is now more compelling than ever that a new class of integrated hydrothermal flux studies be pursued. Sophisticated technological capabilities have now been developed with which we could undertake systematic mapping and characterization to locate all different forms of seafloor fluid flow at the scale of an individual hydrothermally active ridge segment or seamount (e.g. using the AUV *Sentry*), and then to conduct targeted sampling of those systems, using novel and dedicated deepwater robots such as the CLIO vehicle (Breier et al., 2020), in concert with established CTD-rosette approaches to conduct detailed biogeochemical process studies (Fig. 13). Further, if we were to implement such a program embedded within the long-term infrastructure afforded by modern seafloor observatories, we could combine such comprehensive biogeochemical sampling and analyses with state-of-the-art physical oceanographic modeling (e.g. Xu and Lavelle, 2017; Xu and German, 2023) to constrain what the integrated fluxes might be from hydrothermal systems in diverse geological settings, to global ocean biogeochemistry.

Exploring for seafloor hydrothermal venting (and life?) beyond Earth

Perhaps the most surprising of all the remarkable discoveries in the field of submarine hydrothermal processes over the past decade were not made in Earth's oceans at all, but on Enceladus, a tiny moon of Saturn, as part of NASA's Cassini mission (Schenk et al., 2018). At Enceladus' south pole, geysers of frozen ice issue from four major fissures in that planet's geologically-young ice-shell, from what is believed to be a global-scale underlying ocean (Porco et al., 2014; Thomas et al., 2016). Over the past decade, a series

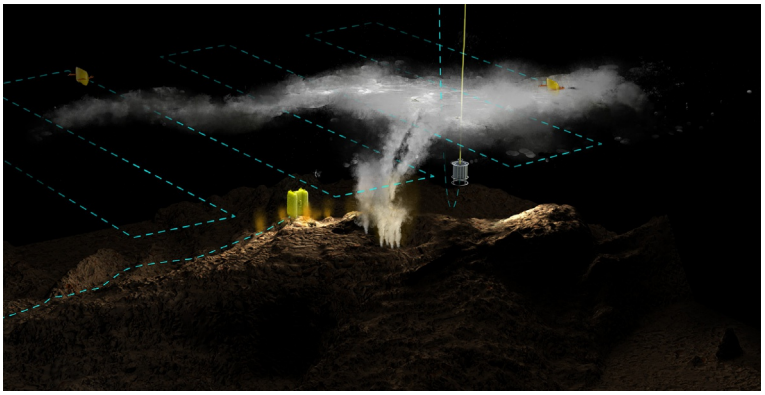

Fig. 13 Schematic of techniques for investigating biogeochemical processes associated with seafloor hydrothermal systems. A CTD-rosette, lowered via cable from a research ship (as shown at center right) has been a mainstay of hydrothermal plume investigations for decades. More recently, increasing attention has turned to the potential use of advanced autonomous vehicles. Two examples illustrated here are the *Sentry* AUV and the *CLIO* system. *Sentry* can be pre-programmed to fly at non-buoyant plume height, to map out lateral anomalies using in situ sensing, and to collect discrete samples for biogeochemical analyses within dispersing non-buoyant plumes (~100 m altitude). *Sentry* can also fly close above the seafloor (~5 m altitude) to identify where locales of lower-temperature flow, out of chemical (redox) equilibrium with the surrounding ocean, are situated. However, *Sentry* cannot loiter so close to the seafloor without risk in such hazardous terrain, and neither can CTD-rosettes safely be lowered so close to the seabed from thousands of meters above. Instead, sampling of this low temperature flow is best pursued using the new *CLIO* vehicle in terrain-following mode, which will allow it to loiter close above the seafloor and activate its sampling devices whenever triggered by the detection of in situ thermal±redox anomalies from its sensors.

of studies using data from in situ instruments that were mounted onboard the Cassini spacecraft, have investigated both the jets of frozen ocean water emitted into those geyser-plumes and the frozen ice-particles transported further, into Saturn's *E*-ring. First, Hsu et al. (2015) identified frozen silica nanoparticles in Saturn's E-ring that they attributed to the presence of some form of submarine venting at Enceladus' seafloor, at temperatures close to 100 °C. Later, during one of Cassini's last "Extended Mission" flybys, it was determined that Enceladus' plumes also contained co-existing H_2, CO_2, and CH_4, providing evidence that Enceladus might host ultramafic-influenced hydrothermal activity akin to modern forms of submarine venting that had only just been discovered on Earth (Seewald, 2017; Waite et al., 2017). Importantly, these novel sites of venting in Earth's oceans – the nearest analogs to Enceladus' inferred hydrothermal activity – have now been shown to have the capacity to host abiotic organic synthesis (Lang et al., 2010; McDermott et al., 2015). This was not known to be possible on Earth at the time that the Cassini mission was launched into space in 1997! With the even more recent determination that Enceladus' plumes also contain abundant organic molecules (Postberg et al., 2018), it now seems clear that Enceladus may not only be habitable but, potentially, inhabited (Cable et al., 2021).

In recognition of these exciting discoveries, the National Academies' recent decadal report to NASA for Planetary Sciences and Astrobiology (NASEM, 2022) has recommended that new missions be pursued urgently, at the New Frontiers and/or Flagship level, to investigate whether submarine venting and associated chemosynthesis could be hosting life on ocean worlds beyond Earth – for example through the Enceladus Orbi-Lander mission concept (MacKenzie et al., 2021, 2022). Separately, four of the five moons of Uranus – designated targets of the complementary Uranus Orbiter and Probe mission concept – have also now been shown to be putative ocean worlds (Castillo-Rogez et al., 2023). Even before development of such missions can begin, however, analyses of complementary data from the Jupiter system have revealed that one of its ocean world moons, Europa (which also hosts a rocky seafloor) may also be emitting geysers of frozen ocean water, similar to Enceladus (Roth et al., 2014; Sparks et al., 2016; Jia et al., 2018). This is potentially even more exciting, if true, because NASA's Flagship *Europa Clipper* mission is scheduled for launch in October 2024 and will conduct multiple fly-pasts of Europa to assess its habitability during the decade ahead. If plumes are located there, the Europa Clipper mission could be extended to intercept and analyze them. To close, therefore, it is interesting to reflect that perhaps the most profound question that submarine hydrothermal research can help us prepare to answer in the coming decades might be: ***Does submarine venting exist on other ocean worlds and, assuming so, do any of those sites host life beyond Earth, right here in our own solar system?***

Summary and outlook

Less than 50 years since their first discovery, hydrothermal vents have been located and sampled in every ocean basin on Earth, from the Arctic to the Southern Ocean. Continuing exploration has revealed an ever-expanding diversity of geological regimes under which hydrothermal circulation can arise and this requires continuous re-evaluation of the impacts that submarine venting might have on marine biogeochemistry from the local to global scale. One paradigm-shifting discovery from the past decade has been that ultramafic-hosted hydrothermal systems can release fluids rich in dissolved hydrogen, which leads to de novo abiotic organic synthesis and can feed diverse, energy-rich microbial ecosystems at and beneath the seafloor. This and related discoveries have facilitated a renaissance of exploration into the organic geochemistry of hydrothermal systems. A second major discovery in the past

Fig. 14 In remembrance. Left: Dr. Harry Elderfield (1943–2016). Center: Dr. Jan Amend (1964–2024). Right: Dr. Diane Poehls Adams (1979–2017).

decade has been the role that hydrothermal plumes play in modifying chemical fluxes from hydrothermal vents to the open ocean. For example, iron released into hydrothermal plumes can be dispersed across entire ocean basins and, potentially, persist over long enough time scales to upwell to the surface ocean at high latitudes where it could, as an essential micronutrient, serve to fertilize growth of iron-limited phytoplankton. This would provide a mechanism by which seafloor hydrothermal fluxes could facilitate carbon sequestration from the atmosphere, a core illustration of how submarine vents can influence not just local ocean chemistry but global-scale biogeochemistry. Key technological advances over the past decade have provided new mechanisms to search systematically for sources of low-temperature hydrothermal flow in addition to the plumes generated by high-temperature venting. Consequently, the decade ahead offers a new opportunity to conduct integrated, systematic quantification of biogeochemical fluxes across a complete hydrothermal field in ways that have hitherto been unattainable. Finally, recent studies have revealed multiple moons in our outer solar system that host liquid water oceans, and on at least two of these moons (Jupiter's Europa and Saturn's Enceladus) those salty oceans are in contact with a rocky seafloor. Should water-rock interactions there establish chemical disequilibria akin to modern Earth's hydrothermal systems, those moons could be habitable – and perhaps inhabited. Future hydrothermal exploration could be the key to a search for life beyond Earth that could be completed within the next human generation.

Remembrance

The hydrothermal community has lost three pioneers in recent years. A synthesizing approach to considering the impacts of submarine venting at the global scale was pioneered by Harry Elderfield (University of Cambridge) a decade before the Treatise of Geochemistry was first published (Elderfield and Schultz, 1996). Jan Amend (University of Southern California) led the field in applying rigorous thermodynamic approaches to investigating the geomicrobiology of hydrothermal systems (Amend et al., 2011; Amend and Shock, 2001). Perhaps nobody played a more pioneering role than Diane Adams (Rutgers University) in exploring how widely the multiple facets of Earth-Ocean processes might interact to shape the influence of submarine venting, from atmospherically-forced eddy circulation to seafloor sedimentation (Adams et al., 2011). We remember them all for the passion and insights that they brought to their research. Their inspiration and their influence endures (Fig. 14).

Acknowledgments

The authors thank Natalie Renier (WHOI) and Isaac Keohane (Univ. South Carolina) for assistance with Figs. 6–8 and 13 and Derrick Hasterok (U.Adelaide) and Stace Beaulieu (WHOI) for providing the data for us to generate new versions of Figs. 1 and 4, respectively.
CRG acknowledges grants: NSF-OCE 1851007 and NASA-80NSSC19K1427.
SQL acknowledges grants: NSF-OCE 1921654, 1801036 and NASA-80NSSC19M0069.
JNF acknowledges grants: NSF-OCE 1737167, 1851078, 2023206, and 2049241.

References

Adams DK, McGillicuddy DJ, Zamudio L, Thurnherr AM, Liang X, Rouxel O, German CR, and Mullineaux LS (2011) Surface-generated mesoscale eddies transport deep-sea products from hydrothermal vents. *Science* 332: 580–583.
Adams DK, Arellano SM, and Govenar B (2012) Larval dispersal: Vent life in the water column. *Oceanography* 25: 256–268.
Alt JC, Scwarzenbach EM, Fruh-Green GL, Shanks WC III, Bernasconi SM, Garrido CJ, Crispini L, Gaggero L, Padron-Navarta JA, and Marchesi C (2013) The role of serpentinites in cycling of carbon and sulfur: Seafloor serpentinization and subduction metamorphism. *Lithos* 178: 40–54.

Amend JP, McCollom TM, Hentscher M, and Bach W (2011) Catabolic and anabolic energy for chemolithoautotrophs in deep-sea hydrothermal systems hosted in different rock types. *Geochimica et Cosmochimica Acta* 75: 5736–5748.

Amend JP and Shock EL (2001) Energetics of overall metabolic reactions of thermophilic and hyperthermophilic Archaea and Bacteria. *FEMS Microbiology Reviews* 25: 175–243. https://doi.org/10.1111/j.1574-6976.2001.tb00576.x.

Ardyna M, Lacour L, Sergi S, d'Ovidio F, Sallée J-B, Rembauville M, Blain S, Tagliabue A, Schlitzer R, and Jeandel C (2019) Hydrothermal vents trigger massive phytoplankton blooms in the Southern Ocean. *Nature Communications* 10(1): 1–8.

Baker ET and German CR (2004) On the global distribution of hydrothermal vent fields. *Geophysical Monograph* 148: 245–266.

Baker ET, German CR, and Elderfield H (1995) Hydrothermal plumes: Global distributions and geological inferences. *Geophysical Monograph* 91: 47–71.

Baker ET, Lavelle JW, Feely RA, Massoth GJ, Walker SL, and Lupton JE (1989) Episodic venting of hydrothermal fluids from the Juan de Fuca Ridge. *Journal of Geophysical Research* 94: 9237–9250. https://doi.org/10.1029/JB094iB07p09237.

Baker ET, Chen YJ, and Morgan JP (1996) The relationship between near-axis hydrothermal cooling and the spreading rate of mid-ocean ridges. *Earth and Planetary Science Letters* 142: 137–145.

Baker ET, Edmonds HN, Michael PJ, Bach W, Dick HJB, Snow JE, Walker SL, Banerjee NR, and Langmuir CH (2004) Hydrothermal venting in magma deserts: The ultraslow-spreading Gakkel and Southwest Indian Ridges. *Geochemistry, Geophysics, Geosystems* 5: Q08002.

Baker ET, Resing JA, Haymon RM, Tunnicliffe V, Lavelle JW, Martinez F, Ferrini V, Walker SL, and Nakamura K (2016) How many vent fields? New estimates of vent field populations on ocean ridges from precise mapping of hydrothermal discharge locations. *Earth and Planetary Science Letters* 449: 186–196. https://doi.org/10.1096/j.epsl.2016.05.031.

Baker ET, Walker SL, Massoth GJ, and Resing JA (2019) The NE Lau basin: Widespread and abundant hydrothermal venting in the back-arc region behind a superfast subduction zone. *Frontiers in Marine Science* 6. https://doi.org/10.3389/fmars.2019.00382.

Baross JA, Anderson RE, and Stueken E (2019) The environmental roots of the origin of life. In: Meadows V, et al. (eds.) *Planetary Astrobiology*, pp. 71–92. Tucson: U. Arizona.

Baumberger T, Lilley MD, Resing JA, Lupton JE, Baker ET, Butterfield DA, Olson EJ, and Fruh-Green GL (2014) Understanding a submarine eruption through time series hydrothermal plume sampling of dissolved and particulate constituents: West Mata, 2008-2012. *Geochemistry, Geophysics, Geosystems* 15: 4631–4650.

Baumberger T, Früh-Green GL, Thorseth IH, Lilley MD, Hamelin C, Bernasconi SM, Okland IE, and Pedersen RB (2016) Fluid composition of the sediment-influenced Loki's Castle vent field at the ultra-slow spreading Arctic Mid-Ocean Ridge. *Geochimica et Cosmochimica Acta* 187: 156–178.

Beaulieu SE and Szafranski K (2020) InterRidge global database of active submarine hydrothermal vent fields Version 3.4. *PANGAEA*. https://doi.org/10.1594/PANGAEA.917894.

Beaulieu SE, Baker ET, German CR, and Maffei A (2013) An authoritative global database for active submarine hydrothermal vent fields. *Geochemistry, Geophysics, Geosystems* 14: 4892–4905.

Beaulieu SE, Baker ET, and German CR (2015) Where are the undiscovered hydrothermal vents on oceanic spreading ridges? *Deep Sea Research, Part II* 121: 202–212.

Bemis K, Lowell RP, and Farough A (2012) Diffuse flow on and around hydrothermal vents at mid-ocean ridges. *Oceanography* 25: 182–191.

Bennett SA, Achterberg EP, Connelly DP, Statham PJ, Fones GR, and German CR (2008) The distribution and stabilization of dissolved Fe in deep-sea hydrothermal plumes. *Earth and Planetary Science Letters* 270: 157–167.

Bennett SA, Rouxel O, Schmidt K, Garbe-Schonberg D, Statham PJ, and German CR (2009) Iron isotope fractionation in a buoyant hydrothermal plume, 5S Mid-Atlantic Ridge. *Geochimica et Cosmochimica Acta* 73: 5619–5634.

Bennett SA, Hansmann RL, Sessions AL, Nakamura K, and Edwards KJ (2011) Tracing iron-fuelled microbial carbon production within the hydrothermal plume at the Loihi seamount. *Geochimica et Cosmochimica Acta* 75: 5526–5539.

Bischoff JL (1969) Red Sea geothermal brine deposits: Their mineralogy, chemistry, and genesis. In: Degens ET and Ross DA (eds.) *Hot Brines Recent Heavy Metal Deposits Red Sea*, pp. 368–401. New York: Springer Verlag.

Bischoff JL and Dickson FW (1975) Seawater-basalt interaction at 200C and 500 Bars – Implications for Origin of Sea-floor heavy metal deposits and regulation of seawater chemistry. *Earth and Planetary Science Letters* 25: 385–397.

Bischoff JL and Seyfried WE (1978) Hydrothermal Chemistry of Seawater from 25 to 350°C. *American Journal of Science* 278: 838–860.

Boettcher M, Roland E, Warren J, Evans R, and Collins J (2023) Observing a seismic cycle at sea. *Eos* 104. https://doi.org/10.1029/2023EO230076.

Bonatti E, Honnorez-Guerstein MB, Honnorez J, and Stern C (1976) Hydrothermal pyrite conretions from the Romanche Trench (Equatorial Atlantic): Metallogenesis in oceanic fracture zones. *Earth and Planetary Science Letters* 32: 1–10.

Bonnet S, Guieu C, Taillandier V, Boulart C, Bouruet-Aubertot P, Gazeau F, Scalabrin C, Bressac M, Knapp AN, Cuypers Y, González-Santana D, Forrer HJ, Grisoni J-M, Grosso O, Habasque J, Jardin-Camps M, Leblond N, Le Moigne FAC, Lebourges-Dhaussy A, Lory C, Nunige S, Pulido-Villena E, Rizzo AL, Sarthou G, and Tilliette C (2023) Natural iron fertilization by shallow hydrothermal sources fuels diazotroph blooms in the ocean. *Science* 380(6647): 812–817. https://doi.org/10.1126/science.abq4654.

Boström K, Peterson MNA, Joensuu O, and Fisher DE (1969) Aluminum-poor ferromanganoan sediments on active ocean ridges. *Journal of Geophysical Research* 74: 3261–3270.

Bourbonnais A, Lehmann MF, Butterfield DA, and Juniper SK (2012) Subseafloor nitrogen transformations in diffuse hydrothermal vent fluids of the Juan de Fuca Ridge evidenced by the isotopic composition of nitrate and ammonium. *Geochemistry, Geophysics, Geosystems* 13: 1–23.

Boyle E, Zurbrick C, Lee J-M, Till R, Till CP, Zhang J, and Flegal AR (2020) Lead and lead isotopes in the U.S. GEOTRACES East Pacific zonal transect (GEOTRACES GP16). *Marine Chemistry* 227: 103892. https://doi.org/10.1016/j.marchem.2020.103892.

Breier JA, Jakuba MV, Saito MA, Dick GJ, Grim SL, Chan EW, McIlvin MR, Moran DM, Alanis BA, Allen AE, and Dupont CL (2020) Revealing ocean-scale biochemical structure with a deep-diving vertical profiling autonomous vehicle. *Science Robotics* 5: eabc7104.

Broecker WS and Peng TH (1982) *Tracers in the Sea*. Palisades, New York: Lamont-Doherty Geological Observatory, Columbia University.

Buck KN, Sedwick PN, Sohst B, and Carlson CA (2018) Organic complexation of iron in the eastern tropical South Pacific: Results from US GEOTRACES Eastern Pacific Zonal Transect (GEOTRACES cruise GP16). *Marine Chemistry* 201: 229–241. https://doi.org/10.1016/j.marchem.2017.11.007.

Butterfield DA, McDuff RE, Mottl MJ, Lilley MD, Lupton JE, and Massoth GJ (1994) Gradients in the composition of hydrothermal fluids from the Endeavour segment vent field: Phase separation and brine loss. *Journal of Geophysical Research* 99: 9561–9583.

Butterfield DA, Nakamura K, Takano B, Lilley MD, Lupton JA, and Roe KK (2011) High SO_2 flux, sulfur accumulation, and gas fractionation at an erupting submarine volcano. *Geology* 39: 803–806.

Byrne RH (2002) Inorganic speciation of dissolved elements in seawater: The influence of pH on concentration ratios. *Geochemical Transactions* 3: 11–16. https://doi.org/10.1039/b109732f.

Cable ML, Porco C, Glein CR, German CR, MacKenzie SM, Neveu M, Hoehler TM, Hofmann AE, Hendrix AR, Eigenbrode J, Postberg F, Spilker LJ, McEwen A, Khawaja N, Waite JH, Wurz P, Helbert J, Anbar A, de Vera J, and Núñez J (2021) The science case for a return to Enceladus. *Planetary Science Journal* 2: 132. https://doi.org/10.3847/PSJ/abfb7a.

Campbell AC, Bowers TS, Measures CI, Falkner KK, Khadem M, and Edmond JM (1988) A time-series of vent fluid compositions from 21°N East Pacific Rise (1979, 1981, 1985) and the Guaymas Basin, Gulf of California (1982, 1985). *Journal of Geophysical Research* 93: 4537–4549.

Campbell AC, German CR, Palmer MR, Gamo T, and Edmond JM (1994) Chemistry of hydrothermal fluids from the Escanaba Trough, Gorda Ridge. *Bulletin. United States Geological Survey* 2022: 201–221.

Castillo-Rogez J, Weiss B, Beddingfield C, Biersteker J, Cartwright R, Goode A, Melwani Daswani M, and Neveu M (2023) Compositions and interior structures of the large moons of Uranus and implications for future spacecraft observations. *Journal of Geophysical Research* 128. https://doi.org/10.1029/2022JE007432.

Chan EW, Alanis BA, German CR, Lim DSS, and Breier JA (2023) Oxygen and deuterium isotopic evidence that Lo'ihi Seamount hydrothermal systems are recharged by Pacific Deep Water. *Deep Sea Research* 197. https://doi.org/10.1016/j.dsr.2023.104049.

Charlou JL, Donval JP, Konn C, Ondreas H, and Fouquet Y (2010) High production and fluxes of H_2 and CH_4 and evidence of abiotic hydrocarbon synthesis by serpentinization in ultramafic-hosted hydrothermal systems on the Mid-Atlantic Ridge. *Geophysical Monograph* 188: 265–296.

Chen S, Tao C, and German CR (2020) Abundance of low-temperature axial venting at the equatorial East Pacific Rise. *Deep Sea Research*. https://doi.org/10.1016/j.dsr.2020.103426.

Chiba H, Masuda H, Lee SY, and Fujioka K (2001) Chemistry of hydrothermal fluids at the TAG Active Mound, MAR 26°N, in 1998. *Geophysical Research Letters* 28. https://doi.org/10.1029/2000GL012645.

Clarke WB, Beg MA, and Craig H (1969) Excess ^{3}He in the sea: Evidence for terrestrial primordial helium. *Earth and Planetary Science Letters* 6: 213–220.

Cohen NR, Noble AE, Moran DM, McIlvin MR, Goepfert TJ, Hawco NJ, German CR, Horner TJ, Lamborg CH, McCrow JP, Allen AE, and Saito MA (2021) Hydrothermal trace metal release and microbial metabolism in the northeastern Lau Basin of the South Pacific Ocean. *Biogeosciences* 18(19): 5397–5422. https://doi.org/10.5194/bg-18-5397-2021.

Coogan LA and Gillis KM (2018) Low-temperature Alteration of the Seafloor: Impacts on Ocean Chemistry. *Annual Review of Earth and Planetary Sciences* 46: 21–45. https://doi.org/10.1146/annurev-earth-082517-010027.

Corliss JB, Dymond J, Gordon LI, Edmond JM, von Herzen RP, Ballard RD, Green K, Williams D, Bainbridge A, Crane K, and van Andel TH (1979) Submarine thermal springs on the Galapagos rift. *Science* 203: 1073–1083.

Cruse A and Seewald JS (2006) Geochemistry of low-molecular weight hydrocarbons in hydrothermal fluids from Middle Valley, northern Juan de Fuca Ridge. *Geochimica et Cosmochimica Acta* 70: 2073–2092.

Davies SHR and Morgan JJ (1989) Manganese (II) oxidation kinetics on metal oxide surfaces. *Journal of Colloid and Interface Science* 129: 63–77.

Davis AC, Bickle MJ, and Teagle DAH (2003) Imbalance in the oceanic strontium budget. *Earth and Planetary Science Letters* 211: 173–187.

de Ronde CEJ and Stucker VK (2015) Chapter 47 – Seafloor Hydrothermal Venting at Volcanic Arcs and Backarcs. In: *The Encyclopedia of Volcanoes*, 2nd edn, pp. 823–849. Academic Press.

de Ronde CEJ, Chadwick WW Jr, Ditchburn RG, Embley RW, Tunnicliffe V, Baker ET, Walker SL, Ferrini VL, and Merle SM (2015) Molten sulfur lakes of intraoceanic arc volcanoes. In: Rouwet D, Christenson B, Tassi F, and Vandemeulebrouck J (eds.) *Advances in Volcanology: Volcanic Lakes*, pp. 261–288. Berlin: Springer-Verlag. Nemeth, K. (Series Ed.).

Dick H, Lin J, and Schouten H (2003) Ultra-slow spreading – a new class of ocean ridge. *Nature* 426: 405–412.

Dick GJ, Anantharaman K, Baker BJ, Li M, Reed DC, and Sheik CS (2013) The microbiology of deep-sea hydrothermal vent plumes: Ecological and biogeographic linakes to seafloor and water column habitats. *Frontiers in Microbiology* 4. https://doi.org/10.3389/fmicb.2013.00124.

Diehl A and Bach W (2020) MARHYS (MARine Hydrothermal Solutions) Database: A global compilation of marine hydrothermal vent fluid, end member, and seawater compositions. *Geochemistry, Geophysics, Geosystems* 21. https://doi.org/10.1029/2020GC009385.

Diehl A and Bach W (2021) MARHYS Database 2.0. *PANGAEA*. https://doi.org/10.1594/PANGAEA.935649.

Ding K and Seyfried WE Jr (2007) In-situ measurement of pH and dissolved H_2 in mid-ocean hydrothermal fluids at elevated temperatures and pressures. *Chemical Reviews* 107: 601–623.

Ding K, Seyfried WE Jr, Zhang Z, Tivey MK, Von Damm KL, and Bradley AM (2005) The in situ pH of hydrothermal fluids at mid-ocean ridges. *Earth and Planetary Science Letters* 237: 167–174.

Edmond JM, Measures C, McDuff RE, Chan L, Collier R, Grant B, Gordon LI, and Corliss J (1979) Ridge crest hydrothermal activity and the balances of the major and minor elements in the ocean: The Galapagos data. *Earth and Planetary Science Letters* 46: 1–18.

Edmond JM, Von Damm KL, McDuff RE, and Measures CI (1982) Chemistry of hot springs on the East Pacific Rise and their effluent dispersal. *Nature* 297: 187–191.

Edmonds HN and Edmond JM (1995) A three-component mixing model for ridge-crest hydrothermal fluids. *Earth and Planetary Science Letters* 134: 53–67.

Eickenbusch P, Takai K, Sissman O, Suzuki S, Menzies C, Sakai S, Sansjofre P, Tasumi E, Bernasconi SM, Glombitza C, Jorgensen BB, Morono Y, and Lever MA (2019) Origin of short-chain organic acids in serpentinite mud volcanoes of the Mariana Convergent Margin. *Frontiers in Microbiology* 10. https://doi.org/10.3389/fmicb.2019.01729.

Elderfield H and Schultz A (1996) Mid-ocean hydrothermal fluxes and the chemical composition of the ocean. *Annual Review of Earth and Planetary Sciences* 24: 191–224.

Elderfield H, Wheat CG, Mottl MJ, Monnin C, and Spiro B (1999) Fluid and geochemical transport through oceanic crust: A transect across the eastern flank of the Juan de Fuca Ridge. *Earth and Planetary Science Letters* 172: 151–165.

Escartin J, Soule SA, Fornari DJ, Tivey MA, Schouten H, and Perfit MR (2007) Interplay between faults and lava flows in construction of the upper oceanic crust: The East Pacific Rise crest 9°25′-9°58′N. *Geochemistry, Geophysics, Geosystems* 8. https://doi.org/10.1029/2006GC001399.

Feely RA, Massoth GJ, Baker ET, Cowen JP, Lamb MF, and Krogslund KA (1990) The effect of hydrothermal processes on midwater phosphorus distributions in the northeast Pacific. *Earth and Planetary Science Letters* 96. https://doi.org/10.1016/0012-821X(90)90009-M.

Field MP and Sherrell RM (2000) Dissolved and particulate Fe in a hydrothermal plume at 9°45′N, East Pacific Rise: Slow Fe (II) oxidation kinetics in Pacific plumes. *Geochimica et Cosmochimica Acta* 64(4): 619–628. http://www.sciencedirect.com/science/article/pii/S0016703799003336.

Findlay AJ, Estes ER, Gartman A, Yücel M, Kamyshny A, and Luther GW (2019) Iron and sulfide nanoparticle formation and transport in nascent hydrothermal vent plumes. *Nature Communications* 10(1): 1597. https://doi.org/10.1038/s41467-019-09580-5.

Fisher AT and Wheat CG (2010) Seamounts as conduits for massive fluid, heat, and solute fluxes on ridge flanks. *Oceanography* 23: 74–87.

Fitzsimmons JN and Conway TM (2023) Novel insights into marine iron biogeochemistry from iron isotopes. *Annual Review of Marine Science* 15. https://doi.org/10.1146/annurev-marine-032822-103431.

Fitzsimmons JN, Jenkins WJ, and Boyle EA (2014) Distal transport of dissolved hydrothermal iron in the deep South Pacific Ocean. *Proceedings of the National Academy of Sciences* 111(47): 16654–16661.

Fitzsimmons JN, Carrasco GG, Wu J, Roshan S, Hatta M, Measures CI, Conway TM, John SG, and Boyle EA (2015a) Partitioning of dissolved iron and iron isotopes into soluble and colloidal phases along the GA03 GEOTRACES North Atlantic Transect. *Deep Sea Research, Part II* 116: 130–151.

Fitzsimmons JN, Hayes CT, Al-Subiai SN, Zhang R, Morton PL, Weisend RE, Ascani F, and Boyle EA (2015b) Daily to decadal variability of size-fractionated iron and iron-binding ligands at the Hawaii Ocean Time-series Station ALOHA. *Geochimica et Cosmochimica Acta* 171: 303–324. https://doi.org/10.1016/j.gca.2015.08.012.

Fitzsimmons JN, John SG, Marsay CM, Hoffman CL, Nicholas SL, Toner BM, German CR, and Sherrell RM (2017) Iron persistence in a distal hydrothermal plume supported by dissolved-particle exchange. *Nature Geoscience* 10: 195–201. https://doi.org/10.1038/NGEO2900.

Foustoukos DI and Seyfried WE Jr (2007) Quartz solubility in the two-phase and critical region of the NaCl-KCl-H_2O system: Implications for submarine hydrothermal vent systems at 9°50′N East Pacific Rise. *Geochimica et Cosmochimica Acta* 71: 186–201.

Früh-Green GL, Connolly JAD, Plas A, Kelley DS, and Grobety B (2004) Serpentinization of oceanic peridotites: Implications for geochemical cycles and biological activity. The subseafloor Biosphere at Mid-Ocean Ridges. *Geophysical Monograph Series* 144: 119–136. https://doi.org/10.1029/144GM08.

Fryer P (2012) Serpentinite mud volcanism: Observations, processes, and implications. *Annual Review of Marine Science* 4: 345–373.

Fyfe WS, Price NJ, and Thompson AB (1978) Fluids in the Earth's crust: Their significance in metamorphic, tectonic and chemical transport processes. In: *Developments in Geochemistry*, vol. 1. Amsterdam, The Netherlands: Elsevier. 382 pp.

Gamo T, Chiba H, Masuda H, Edmonds HN, Fujioka K, Kodama Y, Nanba H, and Sano Y (1996) Chemical characteristics of hydrothermal fluids from the TAG mound of the Mid-Atlantic Ridge in August 1994: Implications for spatial and temporal variability of hydrothermal activity. *Geophysical Research Letters* 23. https://doi.org/10.1029/96GL02521.

Gartman A and Findlay AJ (2020) Impacts of hydrothermal plume processes on oceanic metal cycles and transport. *Nature Geoscience* 13(6): 396–402. https://doi.org/10.1038/s41561-020-0579-0.

Gartman A, Findlay AJ, and Luther GW (2014) Nanoparticulate pyrite and other nanoparticles are a widespread component of hydrothermal vent black smoker emissions. *Chemical Geology* 366: 32–41.

German CR and Seyfried WE Jr (2014) Hydrothermal processes. In: *Treatise on Geochemistry*, 2nd edn, vol. 8, pp. 191–233. Oxford: Elsevier.

German CR and Von Damm KL (2004) Hydrothermal processes. In: *Treatise on Geochemistry*, 1st edn, vol. 6, pp. 181–222. Oxford: Elsevier.

German CR, Klinkhammer GP, Edmond JM, Mitra A, and Elderfield H (1990) Hydrothermal scavenging of rare-earth elements in the ocean. *Nature* 345: 516–518. https://doi.org/10.1038/345516a0.

German CR, Campbell AC, and Edmond JM (1991a) Hydrothermal scavenging at the Mid-Atlantic Ridge: Modification of trace element dissolved fluxes. *Earth and Planetary Science Letters* 107: 101–114. http://www.sciencedirect.com/science/article/pii/0012821X9190047L.

German CR, Fleer AP, Bacon MP, and Edmond JM (1991b) Hydrothermal scavenging at the Mid-Atlantic Ridge: Radionuclide distributions. *Earth and Planetary Science Letters* 105: 170–181.

German CR, Barreiro BA, Higgs NC, Nelsen TA, Ludford EM, and Palmer MR (1995) Seawater metasomatism in hydrothermal sediments (Escanaba Trough, northeast Pacific). *Chemical Geology* 119: 175–190.

German CR, Richards KJ, Rudnicki MD, Lam MM, Charlou JL, and the FLAME Scientific Party (1998) Topographic control of a dispersing hydrothermal plume. *Earth and Planetary Science Letters* 156: 267–273.

German CR, Livermore RA, Baker ET, Bruguier NI, Connelly DP, Cunningham AP, Morris P, Rouse IP, Statham PJ, and Tyler PA (2000) Hydrothermal plumes above the East Scotia Ridge: An isolated high-latitude back-arc spreading centre. *Earth and Planetary Science Letters* 184: 241–250.

German CR, Thurnherr AM, Knoery J, Charlou JL, Jean-Baptiste P, and Edmonds HN (2010) Heat, volume and chemical fluxes from submarine venting: A synthesis of results from the Rainbow hydrothermal field, 36°N, MAR. *Deep Sea Research* 57. https://doi.org/10.1016/j.dsr.2009.12.011.

German CR, Legendre LL, Sander SG, Niquil N, Luther GW III, Bharati L, Han X, and Le Bris N (2015) Hydrothermal Fe cycling and deep ocean organic carbon scavenging: Model-based evidence for significant POC supply to seafloor sediments. *Earth and Planetary Science Letters* 419: 143–153.

German CR, Petersen S, and Hannington MD (2016a) Hydrothermal exploration of mid-ocean ridges: Where might the largest sulfide deposits be forming? *Chemical Geology* 420: 114–126.

German CR, Casciotti KA, Dutay JC, Heimbürger LE, Jenkins WJ, Measures CI, Mills RA, Obata H, Schlitzer R, Tagliabue A, Turner DR, and Whitby H (2016b) Hydrothermal impacts on trace element and isotope ocean biogeochemistry. *Philosophical Transactions of the Royal Society A* 374. https://doi.org/10.1098/rsta.2016.0035.

German CR, Resing JA, Xu G, Yeo IA, Walker SL, Devey CW, Moffett JW, Cutter GA, Hyvernaud O, and Reymond D (2020) Hydrothermal activity and seismicity at Teahitia Seamount: Reactivation of the Society Islands hotspot? *Frontiers in Marine Science* 7: 73. https://doi.org/10.3389/fmars.2020.00073.

German CR, Reeves EP, Türke A, Diehl A, Albers E, Bach W, Purser A, Ramalho SP, Suman S, Mertens C, Walter M, Ramirez-Llodra E, Schlindwein V, Bünz S, and Boetius A (2022a) Volcanically hosted venting with indications of ultramafic influence at Aurora hydrothermal field on Gakkel Ridge. *Nature Communications*. https://doi.org/10.1038/s41467-022-34014-0.

German CR, Baumberger T, Lilley MD, Lupton JE, Noble AE, Saito M, Thurber AR, and Blackman DK (2022b) Hydrothermal exploration of the southern Chile Rise: Sediment hosted venting at the Chile Triple Junction. *Geochemistry, Geophysics, Geosystems* 23: e2021GC010317. https://doi.org/10.1029/2021GC010317.

Gerringa LJA, Rijkenberg MJA, Slagter HA, Laan P, Paffrath R, Bauch D, Rutgers van der Loeff M, and Middag R (2021) Dissolved Cd, Co, Cu, Fe, Mn, Ni, and Zn in the Arctic Ocean. *Journal of Geophysical Research: Oceans* 126(9): e2021JC017323. https://doi.org/10.1029/2021JC017323.

Glazer BT and Rouxel OJ (2009) Redox speciation and distribution within diverse iron-dominated microbial habitats at Loihi Seamount. *Geomicrobiology Journal* 26: 606–622.

Goldberg ED (1954) Marine geochemistry 1. Chemical scavengers of the Sea. *Journal of Geology* 62: 249–265.

González-Santana D, González-Dávila M, Lohan MC, Artigue L, Planquette H, Sarthou G, Tagliabue A, and Santana-Casiano JM (2021) Variability in iron (II) oxidation kinetics across diverse hydrothermal sites on the northern Mid Atlantic Ridge. *Geochimica et Cosmochimica Acta* 297: 143–157. https://doi.org/10.1016/j.gca.2021.01.013.

Guieu C, Bonnet S, Petrenko A, Menkes C, Chavagnac V, Desboeufs K, Maes C, and Moutin T (2018) Iron from a submarine source impacts the productive layer of the Western Tropical South Pacific (WTSP). *Scientific Reports* 8(1): 9075. https://doi.org/10.1038/s41598-018-27407-z.

Haggerty JA and Fisher JB (1992) Short-chain organic acids in interstitial waters from Mariana and Bonin forearc serpentines: Leg125. In: *Proceedings of Ocean Drilling Program*, pp. 387–395. Scientific Results, 125, College Station, TX: Ocean Drilling Program.

Hajash A (1975) Hydrothermal processes along mid-ocean ridges: An experimental investigation. *Contributions to Mineralogy and Petrology* 53: 205–226.

Hasterok D (2013a) A heat flow based cooling model for tectonic plates. *Earth and Planetary Science Letters* 361: 34–43.

Hasterok D (2013b) Global patterns and vigor of ventilated hydrothermal cicrulation through young seafloor. *Earth and Planetary Science Letters* 380: 12–20.

Hatta M, Measures CI, Roshan S, Wu J, Fitzsimmons JN, Sedwick P, and Morton PL (2015) An overview of dissolved Fe and Mn distributions during the 2010-2011 U.S. GEOTRACES North Atlantic cruises: GEOTRACES GA03. *Deep Sea Research, Part II* 116: 117–129.

Hawkes JA, Connelly DP, Gledhill M, and Achterberg EP (2013) The stabilisation and transportation of dissolved iron from high temperature hydrothermal vent systems. *Earth and Planetary Science Letters* 375: 280–290. https://doi.org/10.1016/j.epsl.2013.05.047.

Hawkes JA, Rossel PE, Stubbins A, Butterfield D, Connelly DP, Achterberg EP, Koschinsky A, Chavagnac V, Hansen CT, and Bach W (2015) Efficient removal of recalcitrant deep-ocean dissolved organic matter during hydrothermal circulation. *Nature Geoscience* 8: 856–860.

Haymon RM (1983) Growth history of hydrothermal black smoker chimneys. *Nature* 301(5902): 695–698.

Ho P, Lee J-M, Heller MI, Lam PJ, and Shiller AM (2018) The distribution of dissolved and particulate Mo and V along the U.S. GEOTRACES East Pacific Zonal Transect (GP16): The roles of oxides and biogenic particles in their distributions in the oxygen deficient zone and the hydrothermal plume. *Marine Chemistry* 201: 242–255. https://doi.org/10.1016/j.marchem.2017.12.003.

Hoffman CL, Nicholas SL, Ohnemus DC, Fitzsimmons JN, Sherrell RM, German CR, Heller MI, Lee J-M, Lam PJ, and Toner BM (2018) Near-field iron and carbon chemistry of non-buoyant hydrothermal plume particles, Southern East Pacific Rise 15°S. *Marine Chemistry* 201: 183–197. https://doi.org/10.1016/j.marchem.2018.01.011.

Hoffman CL, Schladweiler CS, Seaton NCA, Nicholas SL, Fitzsimmons JN, Sherrell RM, German CR, Lam PJ, and Toner BM (2020) Diagnostic morphology and solid-state chemical speciation of hydrothermally derived particulate Fe in a long-range dispersing plume. *ACS Earth and Space Chemistry* 4(10): 1831–1842. https://doi.org/10.1021/acsearthspacechem.0c00067.

Hsu H, Postberg F, Sekine Y, Shibuya T, Kempf S, Horányi M, Juhász A, Altobelli N, Suzuki K, Masaki Y, Kuwatana T, Tachibana S, Sirono S, Moragas-Klostermeyer G, and Sarma R (2015) Ongoing hydrothermal activities within Enceladus. *Nature* 519: 207–210. https://doi.org/10.1038/nature14262.

Huber JA, Butterfield DA, and Baross JA (2002) Temporal changes in archaeal diversity and chemistry in a mid-ocean ridge subseafloor habitat. *Applied and Environmental Microbiology* 68(4): 1585–1594. https://doi.org/10.1128/AEM.68.4.1585-1594.2002.

Humphris SE and Klein F (2018) Progress in deciphering controls on the geochemistry of fluids in seafloor hydrothermal systems. *Annual Review of Marine Science* 10: 315–343. https://doi.org/10.1146/annurev-marine-121916-063233.

Humphris SE and Thompson G (1978) Hydrothermal alteration of oceanic basalts by seawater. *Geochimica et Cosmochimica Acta* 42(1): 107–125. https://doi.org/10.1016/0016-7037(78)90221-1.

Hutnak M, Fisher AT, Harris R, Stein C, Wang K, Spinelli G, Schindler M, Villinger H, and Silver E (2008) Large heat fluid fluxes driven through mid-plate outcrops on ocean crust. *Nature Geoscience* 1: 611–614.

James RH, Green DRH, Stock MJ, Alker BJ, Banerjee NR, Cole C, German CR, Huvenne VAL, Powell AM, and Connelly DP (2014) Composition of hydrothermal fluids and mineralogy of associated chimney material on the East Scotia Ridge back-arc spreading centre. *Geochimica et Cosmochimica Acta* 139: 47–71. https://doi.org/10.1016/j.gca.2014.04.024.

Jenkins WJ, Doney SC, Fendrock M, Fine R, Gamo T, Jean-Baptiste P, Key R, Klein B, Lupton JE, and Newton R (2019) A comprehensive global oceanic dataset of helium isotope and tritium measurements. *Earth System Science Data* 11(2): 441–454.

Jenkins WJ, Hatta M, Fitzsimmons JN, Schlitzer R, Lanning NT, Shiller A, Buckley NP, German CR, Lott DE, Weiss G, Whitmore L, Casciotti K, Lam PJ, Cutter GA, and Cahill KL (2020) An intermediate-depth source of hydrothermal He-3 and dissolved iron in the North Pacific. *Earth and Planetary Science Letters* 539. https://doi.org/10.1016/j.epsl.2020.116223.

Jia X, Kivelson MG, Khurana KK, and Kurth WS (2018) Evidence of a plume on Europa from Galileo magnetic and plasma wave signatures. *Nature Astronomy* 2: 459–464.

John SG, Helgoe J, and Townsend E (2018) Biogeochemical cycling of Zn and Cd and their stable isotopes in the Eastern Tropical South Pacific. *Marine Chemistry* 201: 256–262.
Johnson HP and Pruis MJ (2003) Fluxes of fluid and heat from the oceanic crustal reservoir. *Earth and Planetary Science Letters* 216: 565–574.
Kadko D and Moore W (1988) Radiochemical constraints on the crustal residence time of submarine hydrothermal fluids: Endeavour Ridge. *Geochimica et Cosmochimica Acta* 52: 659–668.
Kadko D, Rosenberg N, Lupton J, Collier R, and Lilley M (1990) Chemical reaction rates and entrainment within the Endeavour Ridge hydrothermal plume. *Earth and Planetary Science Letters* 99(4): 315–335.
Kawaka OE and Simoneit BRT (1987) Survey of hydrothermally-generated petroleums from the Guaymas Basin spreading center. *Organic Geochemistry* 11: 311–328.
Kelley DS and Früh-Green GL (2001) Volatile lines of descent in submarine plutonic environments: Insights from stable isotope and fluid inclusion analyses. *Geochimica et Cosmochimica Acta* 65: 3325–3346.
Kelley DS, Karson JA, Fruh-Green GL, Yoerger DR, Shank TM, Butterfield DA, Hayes JM, Schrenk MO, Olson EJ, Proskurowski G, Jakuba M, Bradley A, Larson B, Ludwig K, Glickson D, Buckman K, Bradley AS, Brazelton WJ, Roe K, Elend MJ, Delacour A, Bernasconi SM, Lilley MD, Baross JA, Summons RE, and Sylva SP (2005) A serpentinite-hosted ecosystem: The Lost City hydrothermal field. *Science* 307: 1428–1434.
Kipp LE, Charette MA, Hammond DE, and Moore WS (2015) Hydrothermal vents: A previously unrecognized source of actinium-227 to the deep ocean. *Marine Chemistry* 177: 583–590.
Kipp LE, Sanial V, Henderson PB, van Beek P, Reyss J-L, Hammond DE, Moore WS, and Charette MA (2018) Radium isotopes as tracers of hydrothermal inputs and neutrally buoyant plume dynamics in the deep ocean. *Marine Chemistry* 201: 51–65. https://doi.org/10.1016/j.marchem.2017.06.011.
Klar JK, James RH, Gibbs D, Lough A, Parkinson I, Milton JA, Hawkes JA, and Connelly DP (2017) Isotopic signature of dissolved iron delivered to the Southern Ocean from hydrothermal vents in the East Scotia Sea. *Geology* 45(4): 351–354.
Klein F, Grozeva NG, and Seewald JS (2019) Abiotic methane synthesis and serpentinization in olivine-hosted fluid inclusions. *PNAS* 116: 17666–17672.
Kleint C, Bach W, Diehl A, Fröhberg N, Garbe-Schönberg D, Hartmann JF, et al. (2019) Geochemical characterization of highly diverse hydrothermal fluids from volcanic vent systems of the Kermadec intraoceanic arc. *Chemical Geology* 528: 119289. https://doi.org/10.1016/j.chemgeo.2019.119289.
Klunder MB, Laan P, Middag R, De Baar HJW, and van Ooijen JC (2011) Dissolved iron in the Southern Ocean (Atlantic sector). *Deep Sea Research Part II: Topical Studies in Oceanography* 58(25–26): 2678–2694. http://www.sciencedirect.com/science/article/pii/S0967064510003413.
Klunder MB, Laan P, Middag R, de Baar HJW, and Bakker K (2012) Dissolved iron in the Arctic Ocean: Important role of hydrothermal sources, shelf input and scavenging removal. *Journal of Geophysical Research* 117(C4): C04014. https://doi.org/10.1029/2011jc007135.
Koschinsky A and Hein JR (2003) Uptake of elements from seawater by ferromanganese crusts: Solid-phase associations and seawater speciation. *Marine Geology* 198: 331–351.
Lang SQ, Butterfield DA, Lilley MD, Paul Johnson H, and Hedges JI (2006) Dissolved organic carbon in ridge-axis and ridge-flank hydrothermal systems. *Geochimica et Cosmochimica Acta* 70: 3830–3842.
Lang SQ, Butterfield DA, Schulte M, Kelley DS, and Lilley MD (2010) Elevated concentrations of formate, acetate and dissolved organic carbon found at the Lost City hydrothermal field. *Geochimica et Cosmochimica Acta* 74: 941–952.
Lang SQ, Früh-Green GL, Bernasconi SM, Brazelton WJ, Schrenk MO, and McGonigle JM (2018) Deeply-sourced formate fuels sulfate reducers but not methanogens at Lost City hydrothermal field. *Scientific Reports* 8: 1–10.
Lang SQ, Osburn MR, and Steen AD (2019) Carbon in the deep biosphere: Forms, fates, and biogeochemical cycling. In: *Deep Carbon: Past to Present*, pp. 480–523.
Lang SQ, Lilley MD, Baumberger T, Früh-Green G, Walker S, Brazelton W, Kelley DS, Elend M, and Mau AJ (2021) Extensive decentralized hydrogen export from the Atlantis Massif. *Geology* 49: 851–856. https://doi.org/10.1130/G48322.1.
Lauer RM, Fisher AT, and Winslow DM (2018) Three-dimensional models of hydrothermal circulation through a seamount network on fast-spreading crust. *Earth and Planetary Science Letters* 501: 138–151.
Lecouevre A, Ménez B, Cannat M, Chavagnac V, and Gérard E (2020) Microbial ecology of the newly discovered serpentinite-hosted Old City hydrothermal field (southwest Indian ridge). *The ISME Journal* 15: 818–832. https://doi.org/10.1038/s41396-020-00816-7.
Li M, Toner BM, Baker BJ, Breier JA, Sheik CS, and Dick GJ (2014) Microbial iron uptake as a mechanism for dispersing iron from deep-sea hydrothermal vents. *Nature Communications* 5: 3192.
Lilley MD and Von Damm KL (2008) Volatile behavior at the 9°50'N hydrothermal field through a full volcanic cycle. *EOS. Transactions of the American Geophysical Union*. B23F-01.
Lilley MD, Butterfield DA, Olson EJ, Lupton JE, Macko SA, and McDuff RE (1993) Anomolous CH_4 and NH_4 concentrations at an unsedimented mid-ocean ridge hydrothermal system. *Nature* 364: 45–47.
Lilley MD, Lupton JE, Butterfield DA, and Olson E (2003) Magmatic events produce rapid changes in hydrothermal vent chemistry. *Nature* 422: 878–881.
Lin HT, Cowen JP, Olson EJ, Amend JP, and Lilley MD (2012) Inorganic chemistry, gas compositions and dissolved organic carbon in fluids from sedimented young basaltic crust on the Juan de Fuca Ridge flanks. *Geochimica et Cosmochimica Acta* 85: 213–227.
Lin YS, Koch BP, Feseker T, Ziervogel K, Goldhammer T, Schmidt F, Witt M, Kellermann MY, Zabel M, Teske A, and Hinrichs KU (2017) Near-surface heating of young rift sediment causes mass production and discharge of reactive dissolved organic matter. *Scientific Reports* 7: 1–10.
Lister CRB (1972) On the thermal balance of a Mid-Ocean Ridge. *Geophysical Journal International* 26: 515–535.
Liu X and Millero FJ (2002) The solubility of iron in seawater. *Marine Chemistry* 77: 43–54.
Lough A, Klar J, Homoky W, Comer-Warner S, Milton J, Connelly D, James R, and Mills R (2017) Opposing authigenic controls on the isotopic signature of dissolved iron in hydrothermal plumes. *Geochimica et Cosmochimica Acta* 202: 1–20. https://doi.org/10.1016/j.gca.2016.12.022.
Lough AJM, Connelly DP, Homoky WB, Hawkes JA, Chavagnac V, Castillo A, Kazemian M, Nakamura K, Araki T, Kaulich B, and Mills RA (2019) Diffuse hydrothermal venting: A hidden source of iron to the ocean. *Frontiers in Marine Science* 6. https://doi.org/10.3389/fmars.2019.00329.
Lough AJM, Tagliabue A, Demasy C, Resing JA, Mellett T, Wyatt NJ, and Lohan MC (2023) Tracing differences in iron supply to the Mid-Atlantic Ridge valley between hydrothermal vent sites: Implications for the addition of iron to the deep ocean. *Biogeosciences* 20: 405–420. https://doi.org/10.5194/bg-20-405-2023.
Lowell RP (2017) A fault-driven circulation model for the Lost City Hydrothermal Field. *Geophysical Research Letters* 44: 2703–2709.
Lowell RP, Houghton JL, Farough A, Craft KL, Larson BI, and Meile CD (2015) Mathematical modelling of diffuse flow in seafloor hydrothermal systems: The potential extent of the subsurface biosphere at mid-ocean ridges. *Earth and Planetary Science Letters* 425: 145–153. https://doi.org/10.1016/j.epsl.2015.05.047.
Lupton JE (1995) Hydrothermal plumes, near and far field. *Geophysical Monograph* 91: 317–346.
Lupton J (1998) Hydrothermal helium plumes in the Pacific Ocean. *Journal of Geophysical Research* 103(C8): 15853–15868. https://doi.org/10.1029/98jc00146.
Lupton JE and Craig H (1981) A major helium-3 source at 15°S on the East Pacific Rise. *Science* 214: 13–18.
Lupton J, et al. (2006) Submarine venting of liquid carbon dioxide on a Mariana Arc volcano. *Geochemistry, Geophysics, Geosystems* 7. https://doi.org/10.1029/2005GC00115.
Luther GW (2005) Manganese (II) oxidation and Mn (IV) reduction in the environment—two one-electron transfer steps versus a single two-electron step. *Geomicrobiology Journal* 22(3–4): 195–203.
Luther GW, Findlay A, MacDonald D, Owings S, Hanson T, Beinart R, and Girguis P (2011) Thermodynamics and kinetics of sulfide oxidation by oxygen: A look at inorganically controlled reactions and biologically mediated processes in the environment. *Frontiers in Microbiology* 2. https://doi.org/10.3389/fmicb.2011.00062.
MacKenzie SM, Neveu M, Davila AF, Lunine JI, Craft KL, Cable ML, Phillips-Lander CM, Hofgartner JD, Eigenbrode JL, Waite JH, Glein CR, Gold R, Greenauer PJ, Kirby K, Bradburne C, Kounaves SP, Malaska MJ, Postberg F, Patterson GW, Porco C, Nunez JI, German C, Huber JA, McKay CP, de Vera JP, Brucato JR, and Spilker LJ (2021) The Enceladus Orbilander mission concept: Balancing return and resources in the search for life. *Planetary Science Journal* 2: 77. https://doi.org/10.3847/PSJ/abe4da.
MacKenzie SM, Neveu M, Davila AF, Lunine JI, Cable ML, Phillips-Lander, Eigenbrode JL, Waite JH, Craft KL, Hofgartner JD, McKay CP, Glein CR, Burton D, Kounaves SP, Mathies RA, Vance SD, Malaska MJ, Gold R, German CR, Soderlund KM, Willis P, Freissinet C, McEwen AS, Brucato JR, de Vera JP, Hoehler TM, and Heldmann J (2022) Science objectives for Flagship-class mission concepts for search for evidence of life at Enceladus. *Astrobiology* 22. https://doi.org/10.1089/ast.2020.2425.

Magdalena Santana-Casiano J, Gonzalez-Davila M, and Millero F (2005) Oxidation of nanomolar levels of Fe(II) with oxygen in natural waters. *Environmental Science and Technology* 39(7): 2073–2079. https://doi.org/10.1021/es049748y.
Martin JH (1990) Glacial-interglacial CO_2 change: The iron hypothesis. *Paleoceanography* 5(1): 1–13.
Martin JH and Fitzwater SE (1988) Iron deficiency limits phytoplankton growth in the north-east Pacific subarctic. *Nature* 331: 341–343.
McCarthy M, Beaupre S, Walker B, Voparil I, Guilderson T, and Druffel E (2011) Chemosynthetic origin of C-14-depleted dissolved organic matter in a ridge-flank hydrothermal system. *Nature Geoscience* 4: 32–36.
McCollom T (2000) Geochemical constraints on primary productivity in submarine hydrothermal vent plumes. *Deep-Sea Research* 47: 85–101.
McCollom TM (2008) Observational, experimental, and theoretical constraints on carbon cycling in mid-ocean ridge hydrothermal systems. *Geophysical Monograph* 178: 193–213.
McCollom TM (2016) Abiotic methane formation during experimental serpentinization of olivine. *Proceedings of the National Academy of Sciences* 113: 13965–13970.
McCollom TM and Seewald JS (2007) Abiotic synthesis of organic compounds in deep-sea hydrothermal environments. *Chemical Reviews* 107: 382–401.
McDermott JM, Seewald JS, German CR, and Sylva SP (2015) Pathways for abiotic organic synthesis at submarine hydrothermal fields. *Proceedings of the National Academy of Sciences* 112: 7668–7672.
McDermott JM, Sylva SP, Ono S, German CR, and Seewald JS (2018) Geochemistry of fluids from Earth's deepest ridge-crest hot-springs: Piccard hydrothermal field, Mid-Cayman Rise. *Geochimica et Cosmochimica Acta* 228: 95–118.
McDermott JM, Sylva SP, Ono S, German CR, and Seewald JS (2020) Abiotic redox reactions in hydrothermal mixing zones: Decreased energy availability for the subsurface biosphere. *Proceedings of the National Academy of Sciences* 117: 20453–20461.
McDermott JM, Parnell-Turner R, Barreyre T, Herrera S, Downing CC, Pittoors NC, Pehr K, Vohsen SA, Dowd WS, Wu JN, Marjanovic M, and Fornari DJ (2022) Discovery of active off-axis hydrothermal vents at 9°54'N East Pacific Rise. *Proceedings of the National Academy of Sciences* 119. https://doi.org/10.1073/pnas.2205602119.
Ménez B, Pisapia C, Andreani M, Jamme F, Vanbellingen QP, Brunelle A, Richard L, Dumas P, and Réfrégiers M (2018) Abiotic synthesis of amino acids in the recesses of the oceanic lithosphere. *Nature* 564: 59–63.
Michard A, Michard G, Stuben D, Stoffers P, Cheminee JL, and Binard N (1993) Submarine thermal springs associated with young volcanoes: The Teahitia vents, Society Islands, Pacific Ocean. *Geochimica et Cosmochimica Acta* 57: 4977–4986.
Milesi VP, Shock E, Seewald JS, Trembath-Reichert E, Sylva S, Huber JA, Lim DSS, and German CR (2023) Multiple parameters enable deconvolution of water-rock reaction paths in low-temperature vent-fluids of the Loihi Seamount. *Geochimica et Cosmochimica Acta* 348: 54–67. https://doi.org/10.1016/j.gca.2023.03.013.
Millero FJ (1998) Solubility of Fe(III) in seawater. *Earth and Planetary Science Letters* 154: 323–329.
Millero FJ, Sotolongo S, and Izaguirre M (1987) The oxidation kinetics of Fe(II) in seawater. *Geochimica et Cosmochimica Acta* 51: 793–801.
Moffett JW and German CR (2018) The U.S. GEOTRACES Eastern Tropical Pacific Transect (GP16). *Marine Chemistry* 201: 1–5. https://doi.org/10.1016/j.marchem.2017.12.001.
Monreal P, Hoffman CL, Moore L, Lang SQ, Resing J, and Bundy RM (2021) The characterization of microbially-produced iron-binding ligands across the mid-cayman rise. *Eos, Transactions of the American Geophysical Union*. B35N-1587.
Moore JK, Doney SC, Glover DM, and Fung IY (2002) Iron cycling and nutrient-limitation patterns in surface waters of the World Ocean. *Deep Sea Research Part II: Topical Studies in Oceanography* 49(1–3): 463–507. http://www.sciencedirect.com/science/article/B6VGC-44MX4DN-M/2/155b715b9a6586cf2b9d7b4614c8ec7e.
Moore WS, Frankle J, Benitez-Nelson C, Früh-Green G, and Lang SQ (2021) Activities of 223Ra and 226Ra in fluids from the Lost City Hydrothermal Field require short fluid residence times. *Journal of Geophysical Research*. https://doi.org/10.1029/2021JC017886.
Morel FMM, Milligan AJ, and Saito MA (2014) 8.5 - Marine bioinorganic chemistry: The role of trace metals in the oceanic cycles of major nutrients. In: Holland HD and Turekian KK (eds.) *Treatise on Geochemistry*, 2nd edn, pp. 123–150. Elsevier. https://doi.org/10.1016/B978-0-08-095975-7.00605-7.
Mottl MJ (1992) Pore waters from serpentinite seamounts in the Mariana and Izu-Bonin forearcs, Leg 125: Evidence for volatiles from the subducting slab. *Proceedings. Ocean Drilling Program. Scientific Results* 125: 373–385.
Mottl MJ (2003) Partitioning of energy and mass fluxes between mid-ocean ridge axes and flanks at high and low temperature. In: Halbach PE, Tunnicliffe V, and Hein JR (eds.) *Energy and Mass Transfer in Marine Hydrothermal Systems*, pp. 271–287. Dahlem University Press.
Mottl MJ and McConachy TF (1990) Chemical processes in buoyant hydrothermal plumes on the East Pacific Rise near 21°N. *Geochimica et Cosmochimica Acta* 54(7): 1911–1927. https://doi.org/10.1016/0016-7037(90)90261-I.
Mottl MJ and Wheat CG (1994) Hydrothermal circulation through mid-ocean ridge flanks: Fluxes of heat and magnesium. *Geochimica et Cosmochimica Acta* 58: 2225–2237.
Mottl MJ, Holland HD, and Corr RF (1979) Chemical exchange during hydrothermal alteration of basalt by seawater—II. Experimental results for Fe, Mn, and sulfur species. *Geochimica et Cosmochimica Acta* 43(6): 869–884. https://doi.org/10.1016/0016-7037(79)90225-4.
Mottl MJ, Wheat G, Baker E, Becker K, Davis E, Feely R, Grehan A, Kadko D, Lilley M, Massoth G, Moyer C, and Sansone F (1998) Warm Springs discovered on 3.5 Ma oceanic crust, eastern flank of the Juan de Fuca Ridge. *Geology* 26: 51–54.
Mottl MJ, McCollom TM, Geoffrey Wheat C, and Fryer P (2022) Chemistry of springs across the Mariana forearc: Carbon flux from the subducting plate triggered by the lawsonite-to-epidote transition? *Geochimica et Cosmochimica Acta*. https://doi.org/10.1016/j.gca.2022.10.029.
NASEM - National Academies of Science, Engineering and Medicine (2022) *Origins, Worlds and Life: A Decadal Strategy for Planetary Science and Astrobiology, 2023–2032*. National Academies Press. https://doi.org/10.17226/26522.
Nealson KH, Tebo BM, and Rosson RA (1988) Occurrence and mechanisms of microbial oxidation of manganese. *Advances in Applied Microbiology* 33(C): 279–318.
Neira NM, Clark JF, Fisher AT, Wheat CG, Haymon RM, and Becker K (2016) Cross-hole tracer experiment reveals rapid fluid flow and low effective porosity in the oceanic crust. *Earth and Planetary Science Letters* 450: 355–365.
Neuholz R, Schnetger B, Kleint C, Koschinsky A, Lettmann K, Sander S, Türke A, Walter M, Zitoun R, and Brumsack H-J (2020) Near-field hydrothermal plume dynamics at Brothers Volcano (Kermadec Arc): A short-lived radium isotope study. *Chemical Geology* 533: 119379.
Nielsen SG, Rehkamper M, Teagle DAH, Butterfield DA, Alt JC, and Halliday AN (2006) Hydrothermal fluid fluxes calculated from the isotopic mass balance of thallium in the ocean crust. *Earth and Planetary Science Letters* 251: 120–133.
Nishioka J, Obata H, and Tsumune D (2013) Evidence of an extensive spread of hydrothermal dissolved iron in the Indian Ocean. *Earth and Planetary Science Letters* 361: 26–33. https://doi.org/10.1016/j.epsl.2012.11.040.
Orcutt BN, Sylvan JB, Knab NJ, and Edwards KJ (2011) Microbial Ecology of the dark ocean above, at, and below the Seafloor. *Microbiology and Molecular Biology Reviews* 75: 361–422.
Palmer MR and Edmond JM (1989) The strontium isotope budget of the modern ocean. *Earth and Planetary Science Letters* 92: 11–26. https://doi.org/10.1016/0012-821X(89)90017-4.
Pavia F, Anderson RF, Vivancos SM, Fleisher MQ, Lam PJ, Lu Y, Cheng H, Zhang P, and Edwards RL (2018) Intense hydrothermal scavenging of 230Th and 231Pa in the deep Southeast Pacific. *Marine Chemistry* 201: 212–228. https://doi.org/10.1016/j.marchem.2017.08.003.
Pavia FJ, Anderson RF, Black EE, Kipp LE, Vivancos SM, Fleisher MQ, Charette MA, Sanial V, Moore WS, Hult M, Lu Y, Cheng H, Zhang P, and Edwards RL (2019) Timescales of hydrothermal scavenging in the South Pacific Ocean from ^{234}Th, ^{230}Th, and ^{228}Th. *Earth and Planetary Science Letters* 506: 146–156. https://doi.org/10.1016/j.epsl.2018.10.038.
Plank T, Kelley KA, Zimmer MM, Hauri EH, and Wallace PJ (2013) Why do mafic arc magmas contain ~4 wt% water on average? *Earth and Planetary Science Letters* 364: 168–179. https://doi.org/10.1016/j.epsl.2012.11.044.
Porco C, DiNino D, and Nimmo F (2014) How the geysers, tidal stresses and thermal emission across the South Polar Terrain of Enceladus are related. *The Astrophysical Journal* 148: 45. https://doi.org/10.1088/0004-6256/148/3/45.

Postberg F, Khawaja N, Abel B, Choblet G, Glein CR, Gudipati MS, Henderson BL, Hsu H, Kempf S, Jlenner F, Moragas-Klostermeyer G, Magee B, Nölle L, Perry M, Reviol R, Schmidt J, Srama R, Stolz F, Tobie G, Trieloff M, and Waite JH (2018) Macromolecular organic compounds from the depths of Enceladus. *Nature* 358: 564–568.
Proskurowski G, Lilley MD, and Brown TA (2004) Isotopic evidence of magmatism and seawater bicarbonate removal at the endeavour hydrothermal system. *Earth and Planetary Science Letters* 225(1–2): 53–61.
Proskurowski G, Lilley MD, Seewald JS, Früh-Green GL, Olson EJ, Lupton JE, Sylva SP, and Kelley DS (2008) Abiogenic hydrocarbon production at lost city hydrothermal field. *Science* 319: 604–607.
Reeves EP, McDermott JM, and Seewald JS (2014) The origin of methanethiol in midocean ridge hydrothermal fluids. *Proceedings of the National Academy of Sciences* 111: 5474–5479.
Resing JA, Baker ET, Lupton JE, Walker SL, Butterfield DA, and Massoth GJ (2009) Chemistry of hydrothermal plumes above submarine volcanoes of the Mariana Arc. *Geochemistry, Geophysics, Geosystems* 10. https://doi.org/10.1029/2008GC002141.
Resing JA, et al. (2011) Active submarine eruption of boninite in the northeastern Lau Basin. *Nature Geoscience* 4: 799–806. https://doi.org/10.1038/ngeo1275.
Resing JA, Sedwick PN, German CR, Jenkins WJ, Moffett JW, Sohst BM, and Tagliabue A (2015) Basin-scale transport of hydrothermal dissolved metals across the South Pacific Ocean. *Nature* 523: 200–203.
Robinson AH, Zhang L, Hobbs RW, Peirce C, and Tong VCH (2020) Magmatic and tectonic segmentation of the intermediate-spreading Costa Rica Rift – a fine balance between magma supply rate, faulting and hydrothermal circulation. *Geophysical Journal International* 222: 132–152.
Rogers AD, Tyler PA, Connelly DP, Copley JT, James RH, Larter RD, Linse K, Mills RA, Naveira-Garabato A, Pancost RD, Pearce DA, Polunin N, German CR, Shank T, Alker B, Aquilina A, Bennett S, Clarke A, Dinley J, Graham AGC, Green D, Hawkes J, Hepburn L, Hilario A, Huvenne VAI, Marsh L, Ramirez-Llodra E, Reid W, Roterman CN, Sweeting C, Thatje S, and Zwirglmaier K (2012) The discovery of a new vent biogeographic province in the Southern Ocean. *PLoS Biology* 10: e1001234. https://doi.org/10.1371/journa;.pbio.1001234.
Roshan S, Wu J, and Jenkins WJ (2016) Long-range transport of hydrothermal dissolved Zn in the tropical South Pacific. *Marine Chemistry* 183: 25–32.
Roshan S, DeVries T, Wu J, John S, and Weber T (2020) Reversible scavenging traps hydrothermal iron in the deep ocean. *Earth and Planetary Science Letters* 542: 116297.
Roth L, Saur J, Retherford KD, Strobel DF, Feldman PD, McGrath MA, and Nimmo F (2014) Transient water vapor at Europa's south pole. *Science* 343: 171–174.
Rouxel O, Shanks WC III, Bach W, and Edwards KJ (2008) Integrated Fe- and S-isotope study of seafloor hydrothermal vents at East Pacific Rise 9-10°N. *Chemical Geology* 252(3–4): 214–227.
Rouxel O, Toner B, Germain Y, and Glazer B (2018) Geochemical and iron isotopic insights into hydrothermal iron oxyhydroxide deposit formation at Loihi Seamount. *Geochimica et Cosmochimica Acta* 220: 449–482.
Rudnicki M and Elderfield H (1992) Helium, radon and manganese at the TAG and Snakepit hydrothermal vent fields, 26 and 23 N, Mid-Atlantic Ridge. *Earth and Planetary Science Letters* 113(3): 307–321.
Rudnicki MD and Elderfield H (1993) A chemical model of the buoyant and neutrally buoyant plume above the TAG vent field, 26 degrees N, Mid-Atlantic Ridge. *Geochimica et Cosmochimica Acta* 57(13): 2939–2957. https://doi.org/10.1016/0016-7037(93)90285-5.
Saito MA, Noble AE, Tagliabue A, Goepfert TJ, Lamborg CH, and Jenkins WJ (2013) Slow-spreading submarine ridges in the South Atlantic as a significant oceanic iron source. *Nature Geoscience* 6: 775–779.
Sander SG and Koschinsky A (2011) Metal flux from hydrothermal vents increased by organic complexation. *Nature Geoscience* 4: 145–150.
Schenk PM, Clark RN, Howett CJA, Verbiscer AJ, and Waite JH (eds.) (2018) *Enceladus and the Icy Moons of Saturn*. University of Arizona Press. 475 pp.
Schrenk M, Huber J, and Edwards K (2010) Microbial provinces in the subseafloor. *Annual Review of Marine Science* 2: 279–304.
Schultz A and Elderfield H (1997) Controls on the physics and chemistry of seafloor hydrothermal circulation. *Philosophical Transactions of the Royal Society A* 355: 387–425.
SCOR Working Group (2007) GEOTRACES - An international study of the global marine biogeochemical cycles of Trace Elements and their Isotopes. *Chemie der Erde* 67: 85–131.
Seewald JS (2017) Detecting molecular hydrogen on Enceladus. *Science* 356: 2–3.
Seewald JS, Seyfried WE, and Thornton EC (1990) Organic-rich sediment alteration – An experimental and theoretical study at elevated temperatures and pressures. *Applied Geochemistry* 5: 193–209.
Seewald J, Cruse AM, and Saccocia PJ (2003) Aqueous volatiles in hydrothermal fluids from the Main Endeavour Field, Northern Juan de Fuca Ridge: Temporal variability following earthquake activity. *Earth and Planetary Science Letters* 216: 575–590.
Seton M, Müller RD, Zahirovic S, Williams S, Wright NM, Cannon J, Whittaker JM, Matthews KJ, and McGirr R (2020) A global data set of present-day oceanic crustal age and seafloor spreading parameters. *Geochemistry, Geophysics, Geosystems* 21(10): e2020GC009214. https://doi.org/10.1029/2020GC009214.
Severmann S, Johnson CM, Beard BL, German CR, Edmonds HN, Chiba H, and Green DRH (2004) The effect of plume processes on the Fe isotope composition of hydrothermally derived Fe in the deep ocean as inferred from the Rainbow vent site, Mid-Atlantic Ridge, 36 degrees 14' N. *Earth and Planetary Science Letters* 225(1–2): 63–76. https://doi.org/10.1016/j.espl.2004.06.001.
Seyfried WE Jr and Bischoff JL (1979) Low-temperature basalt alteration by seawater – experimental study at 70-degrees C and 150 degrees C. *Geochimica et Cosmochimica Acta* 43: 1937–1947.
Seyfried WE Jr and Dibble WE Jr (1980) Seawater-peridotite interaction at 300°C and 500 bars: Implications for the origin of oceanic serpentinites. *Geochimica et Cosmochimica Acta* 44: 309–321.
Seyfried WE Jr and Ding K (1995) Phase equilibria in subseafloor hydrothermal systems: A review of the role of redox, temperature, pH and dissolved Cl on the chemistry of hot spring fluids at mid-ocean ridges. *Geophysical Monograph* 91: 248–273.
Seyfried WE Jr, Pester NJ, Tutolo BM, and Ding K (2015) The Lost City hydrothermal system: Constraints imposed by vent fluid chemistry and reaction path models on subseafloor heat and mass transfer processes. *Geochimica et Cosmochimica Acta* 163: 59–79.
Shah Walter SR, Jaekel U, Osterholz H, Fisher AT, Huber JA, Pearson A, Dittmar T, and Girguis PR (2018) Microbial decomposition of marine dissolved organic matter in cool oceanic crust. *Nature Geoscience* 11: 334–339. https://doi.org/10.1038/s41561-018-0109-5.
Sherrell RM, Field MP, and Ravizza G (1999) Uptake and fractionation of rare earth elements on hydrothermal plume particles at 9°45′N, East Pacific Rise. *Geochimica et Cosmochimica Acta* 63(11–12): 1709–1722. https://doi.org/10.1016/S0016-7037(99)00182-9.
Sherwood Lollar B, Heuer VB, McDermott J, Tille S, Warr O, Moran JJ, Telling J, and Hinrichs KU (2021) A window into the abiotic carbon cycle – Acetate and formate in fracture waters in 2.7 billion year-old host rocks of the Canadian Shield. *Geochimica et Cosmochimica Acta* 294: 296–314.
Sieber M, Conway TM, de Souza G, Hassler CS, Ellwood MJ, and Vance D (2021) Isotopic fingerprinting of biogeochemical processes and iron sources in the iron-limited surface Southern Ocean. *Earth and Planetary Science Letters* 567: 116967.
Sigman DM and Boyle EA (2000) Glacial/interglacial variations in atmospheric carbon dioxide. *Nature* 407: 859–869.
Singh SC, Kent GM, Collier JS, Harding AJ, and Orcutt JA (1998) Melt to mush variation in crustal magma properties at the southern East Pacific Rise. *Nature* 394: 874–878.
Sinha MC and Evans RL (2004) Geophysical constraints upon the thermal regime of the ocean crust. *Geophysical Monograph* 148: 19–62.
Snow JE and Edmonds HN (2007) Ultraslow-spreading ridges: Rapid paradigm changes. *Oceanography* 20: 90–101.
Sparks WB, Hand KP, McGrath MA, Bergeron E, Cracraft M, and Deustua SE (2016) Probing for evidence of plumes on Europa with HST/STIS. *The Astrophysical Journal* 829: 121. https://doi.org/10.3847/0004-637X/829/2/121.
Spiess FN, Macdonald KC, Atwater T, Ballard R, Carranza A, Cordoba D, Cox C, Diaz Garcia VM, Francheteau J, Guerrero J, Hawkins J, Haymon R, Hessler R, Juteau T, Kastner M, Larson R, Luyendyk B, MacDougall JD, Miller S, Normark W, Orcutt J, and Rangin C (1980) East pacific rise: Hot springs and geophysical experiments. *Science* 207: 1421–1433.
Statham PJ, German CR, and Connelly DP (2005) Iron (II) distribution and oxidation kinetics in hydrothermal plumes at the Kairei and Edmond vent sites, Indian Ocean. *Earth and Planetary Science Letters* 236(3–4): 588–596. https://doi.org/10.1016/j.epsl.2005.03.008.
Staudigel H and Hart SR (1983) Alteration of basaltic glass-mechanisms and significance from oceanic-crust seawater budget. *Geochimica et Cosmochimica Acta* 47: 337–350.

Staudigel H, Hart SR, Pile A, Bailey BE, Baker ET, Brooke S, Connelly DP, Haucke L, German CR, Hudson I, Jones D, Koppers AAP, Konter J, Lee R, Pietsch TW, Tebo BM, Templeton AS, Zierenberg R, and Young CM (2006) Vailulu'u Seamount, Samoa: Life and death on an active submarine volcano. *Proceedings of the National Academy of Sciences* 103: 6448–6453.

Steffen JM, Summers BA, Conway TM, Thyng KM, Sherrell RM, German CR, and Fitzsimmons JN (2024) Short residence times for hydrothermally-sourced dissolved iron in the deep ocean. *Nature Geoscience*. in revision.

Stein CA and Stein S (1994) Constraints on hydrothermal heat flux through the oceanic lithosphere from global heat flow. *Journal of Geophysical Research* 99: 3081–3095.

Stein CA and Stein S (2015) Are large oceanic depth anomalies caused by thermal perturbations? In: Foulger GR, Lustrino M, and King SD (eds.) *The Interdisciplinary Earth: A Volume in Honor of Don L. Anderson*, vol. 514. Geological Society of America. https://doi.org/10.1130/2015.2514(12).

Stichel T, Pahnke K, Duggan B, Goldstein SL, Hartman AE, Paffrath R, and Scher HD (2018) TAG plume: Revisiting the hydrothermal neodymium contribution to seawater. *Frontiers in Marine Science* 5. https://doi.org/10.3389/fmars.2018.00096.

Stommel H (1982) Is the South Pacific helium-3 plume dynamically active? *Earth and Planetary Science Letters* 61: 63–67.

Stumm W and Morgan JJ (1996) *Aquatic Chemistry: Chemical Equilibria and Rates in Natural Waters*, 3rd edn. John Wiley & Sons.

Sylvan JB, Pyenson BC, Rouxel O, German CR, and Edwards KJ (2012) Time-series analysis of two hydrothermal plumes at 9°50'N East Pacific Rise reveals distinct, heterogeneous bacterial populations. *Geobiology* 10(2): 178–192. https://doi.org/10.1111/j.1472-4669.2011.00315.x.

Tagliabue A and Resing J (2016) Impact of hydrothermalism on the ocean iron cycle. *Philosophical Transactions of the Royal Society A: Mathematical, Physical and Engineering Sciences* 374(2081): 20150291.

Tagliabue A, Bopp L, Dutay J-C, Bowie AR, Chever F, Jean-Baptiste P, Bucciarelli E, Lannuzel D, Remenyi T, and Sarthou G (2010) Hydrothermal contribution to the oceanic dissolved iron inventory. *Nature Geoscience* 3(4): 252–256.

Tagliabue A, Aumont O, and Bopp L (2014) The impact of different external sources of iron on the global carbon cycle. *Geophysical Research Letters* 41. https://doi.org/10.1002/2013gl059059. 2013GL059059.

Takai K, Nakamura K, Toki T, Tsunogai U, Miyazaki M, Miyazaki J, Hirayama H, Nakagawa S, Nanoura T, and Horikoshi K (2008) Cell proliferation at 112C and isotopically heavy CH4 production by a hyperthermophilic methanogen under high-pressure cultivation. *Proceedings of the National Academy of Sciences* 105: 10949–10954.

Tamsitt V, Drake HF, Morrison AK, Talley LD, Dufour CO, Gray AR, Griffies SM, Mazloff MR, Sarmiento JL, Wang J, and Weijer W (2017) Spiraling pathways of global deep waters to the surface of the Southern Ocean. *Nature Communications* 8: 172. https://doi.org/10.1038/s41467-017-00197-0.

Tebo BM, Bargar JR, Clement BG, Dick GJ, Murray KJ, Parker D, Verity R, and Webb SM (2004) Biogenic manganese oxides: Properties and mechanisms of formation. *Annual Review of Earth and Planetary Sciences* 32: 287–328.

Thibault de Chanvalon A, Luther GW, Oldham VE, Tebo BM, Coffey NR, and Shaw TF (2023) Distribution and stability of Mn complexes in the ocean: Influence of hydrothermal plumes and weather events. *Limnology and Oceanography* 68(2): 455–466. https://doi.org/10.1002/lno.12285.

Thomas PC, Tajeddine R, Tiscareno MS, Burns JA, Joseph J, Loredo TJ, Helfenstein P, and Porco C (2016) Enceladus's measured physical libration requires a global subsurface ocean. *Icarus* 264: 37–47.

Titarenko SS and McCaig AM (2016) Modelling the Lost City hydrothermal field: Influence of topography and permeability structure. *Geofluids* 16: 314–328.

Tolstoy M, Cowen JP, Baker ET, Fornari DJ, Rubin KH, Shank TM, Waldhauser F, Bohnenstiehl DR, Forsyth DW, Holmes RC, Love B, Perfit MR, Weekly RT, Soule SA, and Glazer B (1996) A sea-floor spreading event captured by seismometers. *Science* 314: 1920–2922.

Toner BM, Marcus MA, Edwards KJ, Rouxel O, and German CR (2012) Measuring the form of iron in hydrothermal plume particles. *Oceanography* 25(1): 209–212.

Trefry JH and Metz S (1989) Role of hydrothermal precipitates in the geochemical cycling of vanadium. *Nature* 342(6249): 531–533. https://doi.org/10.1038/342531a0.

Turner JS (1973) *Buoyancy Effects in Fluids*. Cambridge University Press. 367 pp.

Twining BS and Baines SB (2013) The trace metal composition of marine phytoplankton. *Annual Review of Marine Science* 5: 191–215.

Vance D, Teagle DAH, and Foster GL (2009) Variable Quaternary chemical weathering fluxes and imbalances in marine geochemical budgets. *Nature* 458: 493–496.

Von Damm KL (1995) Controls on the chemistry and temporal variability of seafloor hydrothermal fluids. *Geophysical Monograph* 91: 222–248.

Von Damm KL (2000) Chemistry of hydrothermal vent-fluids from 9-10N, East Pacific Rise: "Time zero", the immediate posteruptive period. *Journal of Geophysical Research* 105: 11203–11222.

Von Damm KL and Lilley MD (2004) Diffuse flow hydrothermal fluids from 9°50'N East Pacific Rise: Origin, evolution and biogeochemical controls. *Geophysical Monograph* 144: 245–268.

Von Damm KL, Edmond JL, Grant B, Measures CI, Walden B, and Weiss RF (1985a) Chemistry of submarine hydrothermal solutions at 21°N, East Pacific Rise. *Geochimica et Cosmochimica Acta* 49: 2197–2220.

Von Damm KL, Edmond JM, Measures CI, and Grant B (1985b) Chemistry of submarine hydrothermal solutions at Guaymas Basin, Gulf of California. *Geochimica et Cosmochimica Acta* 49: 2221–2237.

Von Damm KL, Oosting SE, Kozlowski R, Buttermore LG, Colodner DC, Edmonds HN, Edmond JM, and Grebmeier JM (1995) Evolution of East Pacific Rise hydrothermal vent fluids following a volcanic eruption. *Nature* 375: 47–50.

Von Damm KL, Parker CM, Zierenberg RA, Lilley MD, Olson EJ, Clague DA, and McClain JS (2005) The Escanaba Trough, Gorda Ridge hydrothermal system: Temporal stability and subseafloor complexity. *Geochimica et Cosmochimica Acta* 69: 4971–4984.

Waite JH, Glein CR, Perryman RS, Teolis BD, Magee BA, Miller G, Grimes J, Perry ME, Miller KE, Bouquet A, Lunine JI, Brockwell T, and Bolton SJ (2017) Cassini finds molecular hydrogen in the Enceladus plume: Evidence for hydrothermal processes. *Science* 356: 155–159.

Walker S, Baker E, Resing J, Nakamura K-I, and McLain P (2007) A new tool for detecting hydrothermal plumes: An ORP sensor for the PMEL MAPR. In: *AGU Fall Meeting Abstracts, 88*.

Wallace PJ (2005) Volatiles in subduction zone magmas: Concentrations and fluxes based on melt inclusion and volcanic gas data. *Journal of Volcanology and Geothermal Research* 140: 217–240. https://doi.org/10.1016/j.jvolgeores.2004.07.023.

Wang H, Yang Q, Ji F, Lilley MD, and Zhou H (2012) The geochemical characteristics and Fe(II) oxidation kinetics of hydrothermal plumes at the Southwest Indian Ridge. *Marine Chemistry* 134-135: 29–35. https://doi.org/10.1016/j.marchem.2012.02.009.

Wankel SD, Germanovich LN, Lilley MD, Genc G, DiPerna CJ, Bradley AS, Olson EJ, and Girguis PR (2011) Influence of subsurface biosphere on geochemical fluxes from diffuse hydrothermal fluids. *Nature Geoscience* 4: 461–468.

Wheat CG, Jannasch HW, Plan JN, Moyer CL, Sansone FJ, and McMurtry GM (2000) Continuous sampling of hydrothermal fluids from Loihi seamount after the 1996 event. *Journal of Geophysical Research* 105: 19353–19367.

Wheat CG, Hulme SM, Fisher AT, Orcutt BN, and Becker K (2013) Seawater recharge into oceanic crust: IODP Exp 327 Site U1363 Grizzly Bare outcrop. *Geochemistry, Geophysics, Geosystems* 14. https://doi.org/10.1002/ggge.20131.

Wheat CG, Fisher AT, McManus J, Hulme SM, and Orcutt BN (2017) Cool seafloor hydrothermal springs reveal global geochemical fluxes. *Earth and Planetary Science Letters* 476: 179–188.

Wheat CG, Becker K, Villinger HW, Orcutt BN, Fournier T, Hartwell AM, and Paul C (2020a) Subseafloor cross-hole tracer experiment reveals hydrologic properties, heterogeneities, and reactions in slow spreading oceanic crust. *Geochemistry, Geophysics, Geosystems* 21. https://doi.org/10.1029/2019GC008804.

Wheat CG, Seewald JS, and Takai K (2020b) Fluid transport and reaction processes within a serpentinite mud volcano: South Chamorro Seamount. *Geochimica et Cosmochimica Acta* 269: 413–428.

Wilcock WSD, Tolstoy M, Waldhauser F, Garcia C, Tan YJ, Bohnenstiehl DR, Caplan-Auerbach J, Dziak RP, Arnulf AF, and Mann ME (2016) Seismic constraints on caldera dynamics from the 2015 Axial Seamount eruption. *Science* 354: 1395–1399.

Wu J, Wells ML, and Rember R (2011) Dissolved iron anomaly in the deep tropical-subtropical Pacific: Evidence for long-range transport of hydrothermal iron. *Geochimica et Cosmochimica Acta* 75(2): 460–468.

Xu G and German CR (2023) Dispersal of deep-sea hydrothermal plumes at the endeavour segment of the Juan de Fuca Ridge: A multiscale numerical study. *Frontiers in Marine Science* 10. https://www.frontiersin.org/articles/10.3389/fmars.2023.1213470.

Xu G and Lavelle JW (2017) Circulation, hydrography, and transport over the summit of Axial Seamount, a deep volcano in the Northeast Pacific. *Journal of Geophysical Research* 122: 5404–5422. https://doi.org/10.1002/2016JC012464.

Yucel M, Gartman A, Chan CS, and Luther GW (2011) Hydrothermal vents as a kinetically stable source of iron-sulphide-bearing nanoparticles to the ocean. *Nature Geoscience* 4: 367–371.

Zierenberg RA, Fouquet Y, Miller DJ, Bahr JM, Baker PA, Bjerkgård T, Brunner CA, Duckworth RC, Gable R, Gieskes J, Goodfellow WD, Gröschel-Becker HM, Guèrin G, Ishibashi J, Iturrino G, James RH, Lackschewitz KS, Marquez LL, Nehlig P, Peter JM, Rigsby CA, Schultheiss P, Shanks WCIII, Simoneit BRT, Summit M, Teagle DAH, Urbat M, and Zuffa GG (1998) The deep structure of a seafloor hydrothermal deposit. *Nature* 392: 485–488.